Received: 19 January 2021 | Revised: 17 January 2022 | Accepted: 26 January 2022

DOI: 10.1002/gea.21908

RESEARCH ARTICLE

Geoarchaeology An International Journal WILEY

High-performing mortar-based materials from the late imperial baths of Aquileia: An outstanding example of Roman building tradition in Northern Italy

Simone Dilaria[1] | Michele Secco[2] | Marina Rubinich[3] | Jacopo Bonetto[1] | Domenico Miriello[4] | Donatella Barca[4] | Gilberto Artioli[5]

[1]Department of Cultural Heritage, University of Padova, Padova, Italy

[2]Department of Cultural Heritage, Interdepartmental Research Center for the Study of Cement Materials and Hydraulic Binders (CIRCe), University of Padova, Padova, Italy

[3]Department of Humanistic Studies and Cultural Heritage, University of Udine, Udine, Italy

[4]Department of Biology, Ecology and Earth Science, University of Calabria, Rende, Italy

[5]Department of Geosciences, Interdepartmental Research Center for the Study of Cement Materials and Hydraulic Binders (CIRCe), University of Padova, Padova, Italy

Correspondence
Simone Dilaria, Department of Cultural Heritage, University of Padova, Piazza Capitaniato n. 7, 35139, Padova, Italy.
Email: simone.dilaria@unipd.it

Abstract

This study provides the first detailed insight into the composition and properties of structural mortars used in a 4th-century AD bath complex in Aquileia, the emblematic center of Roman culture in Northern Italy. Eighteen mortars, taken from different structures of the site, and three stone samples from the vaulting *opus caementicium* have been analyzed adopting a multianalytical approach integrating optical microscopy, X-ray powder diffraction, X-ray fluorescence, and scanning electron microscopy coupled with energy-dispersive spectroscopy. The properties of the compounds are outstanding, as revealed by the formation of hydraulic phases (i.e., Al-tobermorite and AFm) in most of the samples: the waterproofing capabilities of *cocciopesto* mortars are remarkable, as revealed by the formation of anthropogenic Al-tobermorite (5.5 wt%) in pool coating samples; the lightweight of the vaults was guaranteed by the use of porous *caementa* and pozzolanic volcanic aggregates imported from the Gulf of Naples, as demonstrated by petro-mineralogical features and chemical analysis of major and trace elements. This is the first proven case of trade in these building materials to the north of the Italian peninsula. These outcomes shed new light on the robust technical expertise of local artisans in Aquileia and indicate that the *Cisalpina* province was by no means a peripheral reality in the Roman Empire, as far as mortar-based materials are concerned.

KEYWORDS

Aquileia, *cocciopesto*, Phlegrean and Vesuvian pumices and lavas, pozzolanic reaction, provenance analysis

Scientific editing by Hector Neff.

1 | INTRODUCTION

In the last decades, the interest in the archaeometric investigation of ancient mortar-based materials has increased thanks to the awareness of its potential for the reconstruction of the technical expertise of ancient societies. Most of the research deals with the characterization of antique "recipes," focusing on the pozzolanic aggregates and additives, such as fired-clay fragments, pyroclastic rock clasts, and organic ashes, used to strengthen the cohesion and to waterproof the compounds (Lancaster, 2019). Particular attention is paid to correctly identifying the volcanic aggregates referred to by Vitruvius as *harenae fossiciae* (Vitr., II, 4, 1) and *pulvis puteolanus* (Vitr., II, 6, 1-2; V, 12, 2). The former are fine ashes related to the magmatic activity of the Alban and Sabatini Hills, and they were usually used in the mortar mixtures of Rome (D'Ambrosio et al., 2015; Jackson et al., 2007; Marra et al., 2013); the latter are tuff-pumiceous rocks outcropping in the Phlegean Fields out of the Gulf of Naples, which were widely traded and primarily used for the construction of seawater piers all along the ancient Mediterranean (Brandon et al., 2014; D'Ambrosio et al., 2015; Marra, Anzidei, et al., 2016).

The crucial role played by the Romans in the diffusion of concrete technology is well known. The invention of the *opus caementicium*, an economical, versatile, and durable mortar rubble structure (Ginouvés & Martin, 1985, pp. 51–52), was a decisive achievement for complementing the fervid building activity that Rome undertook along with its rapid expansion in the Mediterranean Sea since the 2nd century B.C. (Mogetta, 2015).

Therefore, most of the analytical studies on mortar-based materials have focused on the key contexts of Roman culture in the central-southern part of Italy, where the best examples are represented by Rome (i.e., Belfiore et al., 2014; Boccalon et al., 2019; Jackson, Ciancio Rossetto, et al., 2011; Jackson, Logan, et al., 2011; Jackson et al., 2010; Schmolder-Veit et al., 2019; Silva et al., 2005) and the Vesuvian sites (i.e., Bonazzi et al., 2007; De Luca et al., 2015; Miriello et al., 2010, 2018; Piovesan et al., 2009; Rispoli et al., 2019, 2020; Secco et al., 2019). Further research concerning towns of the provinces of the Empire has been published in the last decades. These include Sicily and Sardinia, Southern France, North Africa, the Iberian Peninsula, Greece, and Asia Minor (i.e., Alonso-Olazabal et al., 2020; Coutelas, 2012; Degryse et al., 2002; De Luca et al., 2013; Gliozzo & Camporeale, 2009; Miriello et al., 2011; Montana et al., 2018; Papayianni et al., 2013; Secco et al., 2020; Stefanidou et al., 2014).

Provincia Gallia Cisalpina (now corresponding to Northern Italy, Slovenia, and Istria) marks a significant gap in this scenario. Over the past few years, the characterization of structural mortars received little consideration (i.e., Baccelle Scudeler & De Vecchi, 2003; Bugini & Folli, 1993, 2007; Costa et al., 2001), and only recently were the first thorough analytical research articles published (Appolonia et al., 2010; Kramar et al., 2011). An important aspect that can be detected is the substantial absence of any evidence of the use of volcanic *pozzolans* in the mortar-based materials of the region, with few exceptions that, unfortunately, were not confirmed by adequate analysis. The absence of volcanic *pozzolans* could be due to a supply shortage of these products in the region, but this datum could be simply biased by the lack of in-depth analytical studies.

Regarding the *Cisalpina* region, Aquileia, located in today's Friuli Venezia Giulia region (Figure 1a), has been considered a prominent representation of the technical expertise of Roman Northern Italy (Ghedini et al., 2009), and recent analytical research provided new data on the characteristics of mortar-based materials produced in the town in its long history (Dilaria & Secco, 2018; Dilaria et al., 2016, 2019; Secco et al., 2018).

Since its foundation in 181 B.C., Aquileia represented a bridgehead in the spread of the Roman culture to the north of the peninsula. The town developed into a flourishing urban center during the Imperial Age, enriched with monumental buildings and prestigious private houses. In the 4th century AD, Ausonius (Aus. XI, 9, 4) considered Aquileia one of the nine most important and extended cities of the Roman Empire, hosting the Imperial court for some periods. Between the 3rd and 4th century AD, the urban walls were frequently renovated to protect the town from recurring sieges and raids, mirroring a period of great political instability. Indeed, less than one century later, starting from Attila's invasion (452 AD) until the end of the 5th century AD, Aquileia faced an inevitable decline and transformation of the urban space, due to the loss of its political relevance.

2 | THE CASE STUDY

The Late Imperial bath complex of Aquileia is located in the southwestern portion of the Roman town (Figure 1b). The site was first investigated, between 1922 and 1923, by G. Brusin, then by L. Bertacchi in 1961, and by P. Lopreato during the 1980s (Rubinich, 2013, 2014). Owing to its large size (between 22,500 and 25,000 m^2), the building was immediately interpreted as being a bath complex. It was named "Grandi Terme" (literally "Great Baths"), as it was probably one of the largest spas in Roman Italy, comparable with the Baths of Caracalla in Rome (Rubinich, 2018). Since the early 2000s, new excavations to understand its plan have been carried out by the University of Udine and are currently underway under the guidance of Prof. Rubinich (Rubinich, 2014, 2020 and references therein).

Although the exact date of construction is still uncertain, the baths were probably built in the first half of the 4th century AD, as indicated by a dedication to Emperor Constantine by the *praepositi operis*, which were involved in the construction of the so-called *Thermae Felices Constantinianae* (Rubinich, 2013, 2014). A later dating to the mid-4th century AD is suggested by the discovery by Lopreato of a coin of Constantius II (348–350 AD) in the foundation of a mosaic pavement. Given the size of the complex, it is likely that the construction lasted for decades and was completed by Constantine's successors (Rubinich, 2014, 2020).

From a constructive point of view, the entire thermal complex was initially (Phase Ia) built onto an extensive trench above wooden

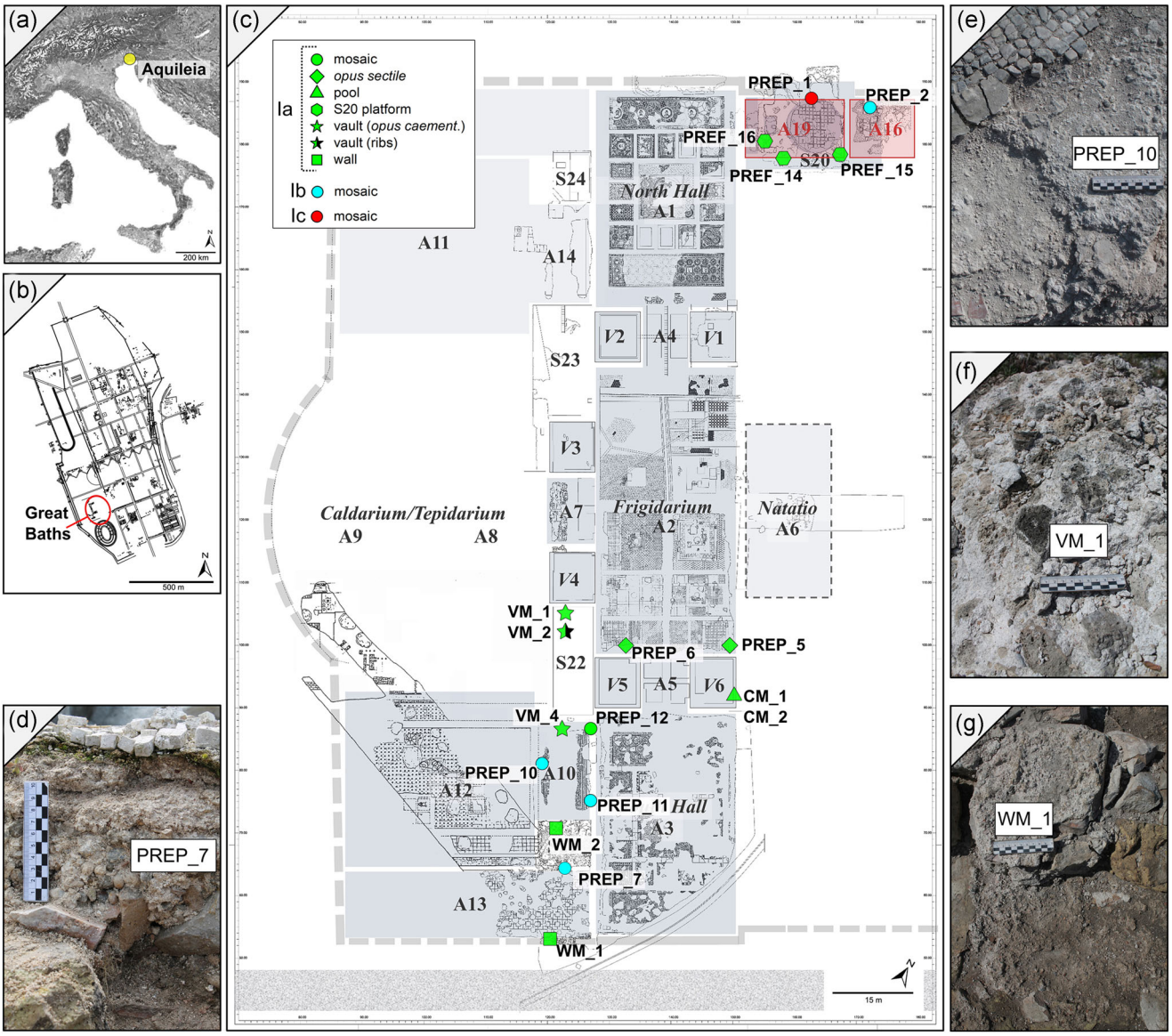

FIGURE 1 Aquileia and the Great Baths. (a) Position of Aquileia in Northern Italy; (b) indication of the site of the Great Baths in the plan of Roman Aquileia; (c) plan of the site after the 2019 excavation with the indication of the position and chronology of the sampled mortar-based materials and the type of structure they come from; and (d–g) selection of sampled structures [Color figure can be viewed at wileyonlinelibrary.com]

pilings fixed into the silty-clayish subsoil of the area. The plan of the complex reflects the typical organization of Roman Imperial *thermae* (Figure 1c), with symmetrical rooms along an N/S axis whose fulcrum is the 45 × 22 m *frigidarium* (room A2), paved in *opus sectile* (Figure 2a). Two equally sized halls (32 × 22 m), respectively A1 (North Hall) and A3 (South Hall), interpreted as *palaestrae-apodyteria*, were located to the north and south of the frigidarium. Six pools, paired two by two, were located to the north, west, and south sides of the frigidarium, while a 20 m wide *natatio* was placed eastwards (Figure 2b). The building was also equipped with a sophisticated system of conduits and hydraulic infrastructures for water adduction (Rubinich, 2018). On the west side, the heated rooms were arranged on suspensurae pavements (A12). Bertacchi's excavations investigated the furnace connected to the heating hypocaust system of the *caldarium*, which was probably closed by a large exedra as revealed by ground penetrating radar prospections. In the NE sector, recent excavations brought to light a large *opus caementicium* (Ginouvés & Martin, 1985, pp. 51–52) platform 13 × 16 (or 20) m, called S20 (Figure 2c), consisting of a base layer of coarse marble fragments and an upper part made of bricks in planar rows bonded with mortar. At least two rectangular basins were installed on the S20 platform, bordering a circular one in the center (Rubinich, 2018, 2020).

Most of the building's floors were in *opus sectile* or mosaic, while little is known about the building techniques and materials, as the masonries were robbed down to their foundations by the massive postantique spoliation activities. The preserved parts showed that most of the load-bearing walls were full-body brick structures (Previato, 2015, pp.

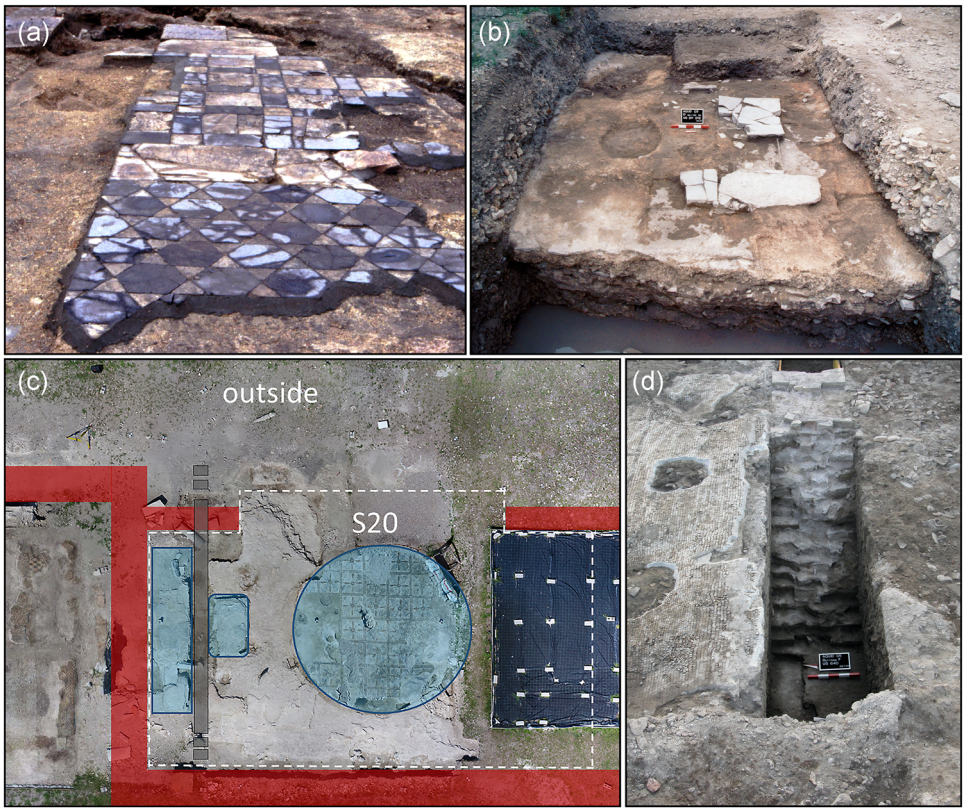

FIGURE 2 Aquileia, Great Baths. (a) *Opus sectile* floor of the *frigidarium* (Lopreato excavation—1987). Archive picture, courtesy of the Ministry of Culture, Regional Direction of the Museums of Friuli Venezia Giulia—National Archaeological Museum of Aquileia, slide 87073; (b) a portion of the floor of the hydraulic basins (*natatio*), east of the *frigidarium* (excavations UniUd—2003); (c) orthophoto of the *opus caementicium* platform S20 (excavation UniUd—2019). The wall trenches are shown in dark red; the profile of the S20 platform is shown as a white dashed line; a N–S drainage channel is shown in gray; the profiles of the tanks or fountains are shown in light blue; and (d) the south boundary wall of the Great Baths made of bricks in planar rows (excavation UniUd—2005) [Color figure can be viewed at wileyonlinelibrary.com]

138–139) (Figure 2d), decorated with painted coatings (Rubinich, 2012a). Vaults constituted the roofing system in *opus caementicium* with brick ribs that were low light-weighted with porous volcanic rocks. Over time, the baths were subjected to several renovations that mainly involved the decorations of floors and walls. Ancient restorations are split into two phases: the first phase dates back to between the late 4th century AD and the early 5th century AD (Phase Ib), while the second phase dates back to the first decades of the 5th century AD (Phase Ic).

Phase Ib refurbishments are particularly evident in the NE sector, where the S20 platform was obliterated by the construction of two rooms (A16, A19), decorated with a big *tesserae* mosaic pavement.

In Phase Ic, two rooms decorated with mosaics (A17–A18) were built over the pavement of room A16 of Phase Ib (Rubinich, 2020).

During the first centuries of the early Middle Ages, some rooms of the bath complex were occupied by small family units that buried their dead out of the southern perimeter wall (A13). Later, the building collapsed and became a large open-air quarry. Since the 13th century, after the systematic removal of the ruins, the site was used exclusively for agricultural purposes and it was surrounded by a thick wall, called "Braida Murada," namely, "urban field enclosed by masonry walls" (Rubinich, 2012b).

3 | SAMPLING

Eighteen mortar samples were collected from different sectors of the Great Baths (Table 1). They were labeled with the name of the site (GTR) according to the function of the structures they come from:

(1) two samples (WM_1 and WM_2) come from joint mortars of full-body brick masonry walls (Figure 1g);
(2) eight samples are of floor bedding screeds (PREP). In detail, two samples come from the screed of the Phase Ia *opus sectile* of the *frigidarium* (PREP_5 and PREP_6) and six from mosaics of Phase Ia (PREP_12), Ib (PREP_2, 7, 10, 11) (Figure 1d,e), and Ic (PREP_1);
(3) three samples are of structural mortars from the S20 *opus caementicium* platform (PREF_14, 15, 16);
(4) two samples represent pool coatings (CM_1 and CM_2); and
(5) three samples come from the collapsed chunks of the vaults. Two of them (VM_1 and 4) have been collected from the *opus caementicium* portion (Figure 1f), while the third comes from the joint mortar of the brick ribs (VM_2).

TABLE 1 Summary of mortars/concretes and rock samples collected from the site of the Great Baths with an indication of the structure they come from and the phase they refer to

Sample	Structure	Phase	Macroscopic description
Mortar and concretes			
GTR_WM_1	Wall	Ia	Cocciopesto
GTR_WM_2	Wall (plint)	Ia	Cocciopesto
GTR_PREP_1	Mosaic floor	Ic	Lime mortar
GTR_PREP_2	Big *tesserae* mosaic	Ib	Lime mortar
GTR_PREP_5	*Opus sectile* floor	Ia	Cocciopesto
GTR_PREP_6	*Opus sectile* floor	Ia (uncertain)	Cocciopesto
GTR_PREP_7	Mosaic floor	Ib	Cocciopesto (up); concrete (down)
GTR_PREP_10	Mosaic floor	Ib	Cocciopesto
GTR_PREP_11	Mosaic floor	Ib	Cocciopesto
GTR_PREP_12	Mosaic floor	Ia	Cocciopesto
GTR_PREF_14	S20 *opus caementicium* platform	Ia	Cocciopesto
GTR_PREF_15	S20 *opus caementicium* platform	Ia	Cocciopesto
GTR_PREF_16	S20 *opus caementicium* platform	Ia	Cocciopesto
GTR_CM_1	Pool	Ia	Cocciopesto
GTR_CM_2	Pool	Ia	Cocciopesto
GTR_VM_1	Vault (*opus caementicium*)	Ia	Cocciopesto
GTR_VM_2	Vault (rib)	Ia	Cocciopesto
GTR_VM_4	Vault (*opus caementicium*)	Ia	Cocciopesto
Lightweight caementa			
GTR_VM_1_G	Vault (*opus caementicium*)	Ia	Volcanic rock
GTR_VM_1_N	Vault (*opus caementicium*)	Ia	Volcanic rock
GTR_VM_4_R	Vault (*opus caementicium*)	Ia	Volcanic rock

In the samples with a stratified structure (i.e., mosaic screeds), each layer has been individually analyzed and labeled with a progressive number, proceeding from the topmost to the lower portion of the sample (i.e., PREP_7.1, 7.2, 7.3).

Furthermore, three stone samples, representing the three lightweight caementa lithotypes used in the vaults, were collected.

4 | ANALYTICAL METHODS

4.1 | Quantitative optical microscopy (OM) and statistical treatment

All mortar and rock samples were subjected to a preliminary petrographic study performed on 30 μm thin sections analyzed under a Nikon Eclipse ME600 microscope.

Mortar analysis was carried out according to the macroscopic and microstratigraphic analytical procedures described in Standard UNI 11176:2006 "Cultural heritage—Petrographic description of a mortar." For each sample (or for each layer in the case of the multilayered sample PREP_7), the rates of binder, porosity, and different aggregates (i.e., fired-clay fraction, sand, etc.) were determined by digital image analysis performed using Image-J software (Schneider et al., 2012). The quantification was performed taking OM-TL scans of the thin sections as the reference; these scans were graphically treated with biochromatic thresholding after transforming the RGB images into 8-bit grayscales (Casadio et al., 2005; Marinoni et al., 2005; Miriello & Crisci, 2006). Porosity and aggregates were quantified separately, while estimation of the binder fraction was performed by subtracting from the total area the sum of aggregates and voids percentages. The size distribution of the aggregate was calculated from the mean of two series of ten manual measurements, representing the diameter of a coarse (usually >2.0 mm) and a fine fraction (<2.0 mm) of the aggregate. The sorting was performed based on the standard deviation (SD) between the mean measurements of fine and coarse aggregates. The mass color was defined

using Munsell soil color charts (Munsell, 1994). To interpret correlation patterns among samples, the petrographic quantitative data were subjected to a multivariate statistical treatment by principal component analysis (PCA). This is a valid procedure for a rough grouping of samples according to their petrographic features (De Luca et al., 2013, 2015; Dilaria, 2020; Miriello et al., 2018). PCA was performed on log-transformed petrographic descriptive variables to obtain a small number of linear combinations that adequately describes the original mortar profiles. A series of principal components representing the data set variability were extracted, according to the following parameters: (i) all the variables were considered for analysis and (ii) no limit was set for the number of principal components to be calculated. Samples were then reported in a scatterplot according to the value of the first two extracted components (PC1, PC2). All statistical analyses were carried out using Statgraphics Centurion PRO 18 software.

4.2 | X-ray powder diffraction (XRPD)

The mineralogical investigations were performed on the three rock samples and on a selection of representative mortars of the groups identified after the PCA treatment of quantified OM data. Mineralogical profiles were determined by quantitative phase analysis based on X-ray powder diffraction (XRPD-QPA). Measurements were obtained using a Bragg–Brentano θ–θ diffractometer (PANalytical X'Pert PRO, Cu-Kα radiation, 40 kV and 40 mA), equipped with a real-time multiple strip (RTMS) detector (X'Celerator by Panalytical). QPA profiles were then determined adopting the same methodology as that described in Secco et al. (2019, 2020).

To properly describe the formation of both geogenic and anthropogenic products, XRPD analyses were carried out on bulk samples (XRPD-*bulk*) and on the separated binder fraction (XRPD-*binder*) of mortars. The latter analysis was performed using the Cryo2Sonic 2.0 separation procedure (Addis et al., 2019), custom-modified through the addition of a chelating agent to the sedimentation solution (sodium hexametaphosphate 0.5 wt%) to favor the suspension of the finer, noncarbonate phases such as clay minerals and hydrate products, prone to flocculation due to their surface charges, as described in Secco et al. (2020).

4.3 | Scanning electron microscopy coupled with energy-dispersive spectroscopy (SEM-EDS)

SEM-EDS analyses were performed on rock sample VM_1_G and on a selection of representative mortars of the groups identified after the PCA treatment of quantified OM data. Microchemical and microstructural analyses were performed using a Camscan MX2500 microscope, equipped with a lanthanum hexaboride source and an EDAX energy-dispersive microanalysis system. The qualitative interpretation of the fluorescence spectra and the semiquantitative estimation of the percentages, by the weights of oxides, were performed using the dedicated software

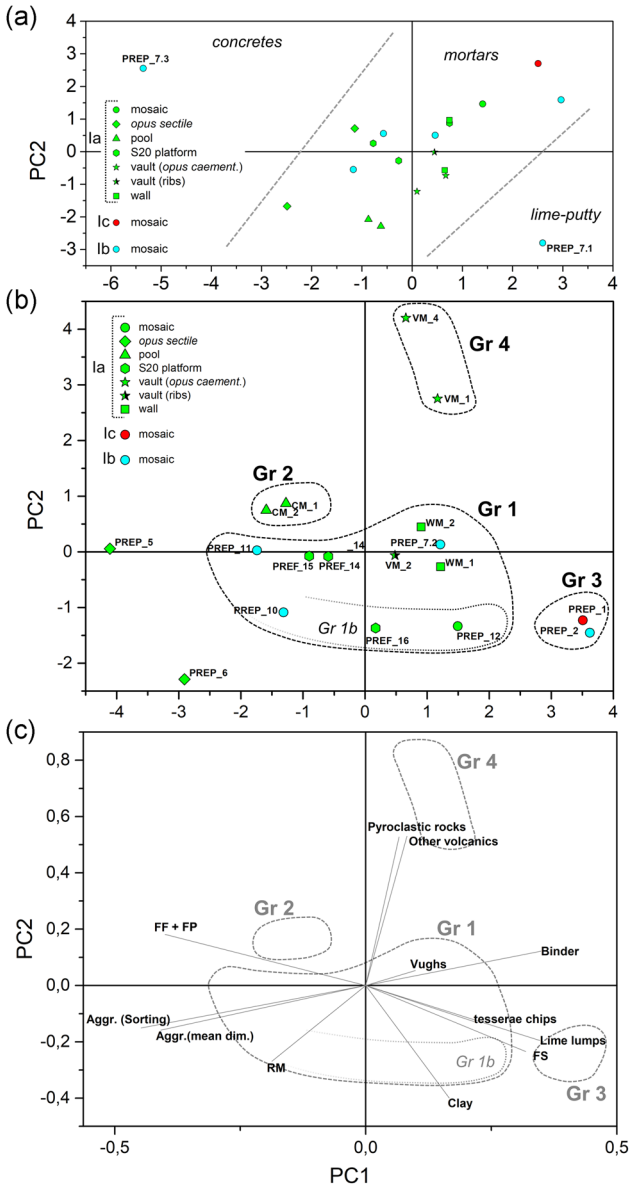

FIGURE 3 Principal component analysis (PCA) graph of optical microscopy quantitative data. The first principal component (PC1) is represented on the *x* axis, and the second principal component is represented on the *y* axis (PC2). (a) PCA distribution based on the full sample/layers data set; (b) PCA distribution of mortar samples/layers and their relative grouping after the exclusion of PREP_7.1 and 7.3; and (c) influence weight of mineral phases, shown as vectors. Gr 1, *cocciopesto* with FS mixed with FF; Gr 1b, *cocciopesto* having FS prevailing on FF; Gr 2, highly cohesive *cocciopesto* with abundant FF and FP; Gr 3, binder-rich lime mortars; Gr 4, *cocciopesto* with volcanic aggregates (lava and pumices) [Color figure can be viewed at wileyonlinelibrary.com]

SEMQuant Phizaf. The SEM-EDS analyses were carried out to (a) analyze the chemical composition of the binders; (b) confirm the distribution of hydraulic phases in the matrices, on the basis of XRPD results (this was done adopting the cementation [*CI*] and hydraulicity [*HI*] indices

in accord with Boynton, 1966); and (c) provide a semiquantitative estimation of major chemical elements of volcanic rock aggregates and *caementa*, to corroborate X-ray fluorescence (XRF) geochemical analyses.

4.4 | XRF

XRF analysis was performed to determine the provenance of the three vaulting *caementa* by comparing their major and trace chemical elements with the data in the literature. The analysis was performed using a Bruker S8 Tiger WD X-ray fluorescence spectrometer with an XRF radius of 34 mm, equipped with a rhodium tube operating at an intensity of 40 kW, following the method for correcting matrix effects of Franzini et al. (1972, 1975). The material for XRF analysis was collected from the core of pluri-centimetric fragments of the *caementa*. We mechanically scraped away the interfacial zones between the rock and the binder in order to avoid intrusion in the analysis, as much as possible (Jackson et al., 2014, p. 186). Samples were analyzed without a preliminary HCl bathing, as this step could affect major and trace elements, in particular Y (D'Ambrosio et al., 2015; Marra, Anzidei, et al., 2016; Marra, D'Ambrosio, et al., 2016).

5 | RESULTS

5.1 | Mortar composition and groups

PCA analysis of quantified OM data was performed to identify groups of mortars having similar features. Because of the high compositional variability, a PCA analysis on the full sample data set was performed to distinguish "concrete" (Ginouvés & Martin, 1985, p. 51) layer PREP_7.3 and a "lime putty" (Ginouvés & Martin, 1985, p. 45) layer PREP_7.1 from the central core, represented by all the other mortars (Figure 3a). A second PCA (PC1 = 34.7% and PC2 = 17.5% of the global variance), performed excluding PREP_7.1 and 7.3, enhanced mortar clustering. Most of the samples are distributed within four groups, while only two are the outliers (Figure 3b,c and Table 2). Gr 1 is the most populated group and it reunites *cocciopesto* mortars (Ginouvés & Martin, 1985, p. 51) having no peculiar features (WM_1, 2, 7.2, PREP_11, PREF_14, 15, VM_2), as they fall in the middle of the scatterplot at PC1 = 0 ± 2 and PC2 = 0 ± 0.5. Three samples having PC2 < −1 (PREP_10, 12, PREF_16) are reunited in a subordinate group (Gr 1b).

Gr 2 reunites samples CM_1 and 2, falling at PC1 < 0 and PC2 > 0.5. They are characterised by the abundance of fired-clay fragments (FF) and fired-clay powder (FP, ⌀ < 0.10 mm).

Gr 3 clusters lime mortars (Ginouvés & Martin, 1985, p. 50) PREP_1 and 2 falling at PC1 > 3. They are strongly correlated in terms of the abundance of clasts of fluvial sediments (FS), lime lumps, and *tesserae* chips.

Gr 4 groups samples VM_1 and 4, falling at PC2 > 2.5. The peculiar feature of these mortars consists of the presence of volcanic rocks as aggregates.

Finally, PREP_5 and PREP_6, both having PC1 < −2.5, are separated from the other groups and they can be considered as outliers.

The main petrographic characteristics of the groups reported hereafter are summarized in Table S3:

(1) Gr 1 samples have moderate toughness and a whitish mass color (2.5 YR 8/3). The aerial lime paste has a micritic texture. The binder-to-aggregate ratio (B/A), ranging between 0.7 and 1.6, is typical for very fat mixtures (Ginouvés & Martin, 1985, p. 50). The aggregate fraction (33%–49%) has a moderate sorting (1.3–2.8 SD) and it is made of FS mixed with FF and sporadic FP (Figure 4a). FS clasts fall in the granulometric range of medium to fine sands (Wentworth, 1922). They are represented by carbonate (≃2/3 of this fraction, with limestones prevailing on dolostones) and silicate (quartz and chert, ≃1/3 of this fraction) granules. Scattered minerals of feldspars (albite) and micas (muscovite) have been detected. The FS/FF + FP ratio ranges from 0.2 to 1.4 (with the only exception of WM_1 having FS/FF + FP = 3.1). Sometimes, reaction rims have been found around FF or FP. The binder matrix is zoned, where the areas having low birefringence color indicate the occurrence of hydrate phases (Pecchioni et al., 2014). Samples of Gr 1b (PREP_10, 12, PREF_16) can be distinguished from those of Gr 1 for an increased presence of

TABLE 2 Sample distribution in groups after PCA analysis on OM quantitative data

Group	Samples (GTR)	Main compositional features
1	WM_1; WM_2; PREP_7.2; PREP_11; PREF_14; PREF_15; VM_2	*Cocciopesto* made of FS mixed with FF with the sporadic presence of FP
1b	PREP_10; PREP_12; PREF_16	*Cocciopesto* having FS prevailing on FF
2	CM_1; CM_2	Highly cohesive *cocciopesto* with abundant FF and diffused FP
3	PREP_1; PREP_2	Binder-rich lime mortars
4	VM_1; VM_4	*Cocciopesto* with volcanic aggregates (lava and pumices)
Outliers	PREP_5; PREP_6; PREP_7.1; PREP_7.3	

Abbreviations: FF, fired-clay fragments; FP, fired-clay powder (⌀ < 0.10 mm); FS, fluvial subrounded sediments; OM, optical microscopy; PCA, principal component analysis.

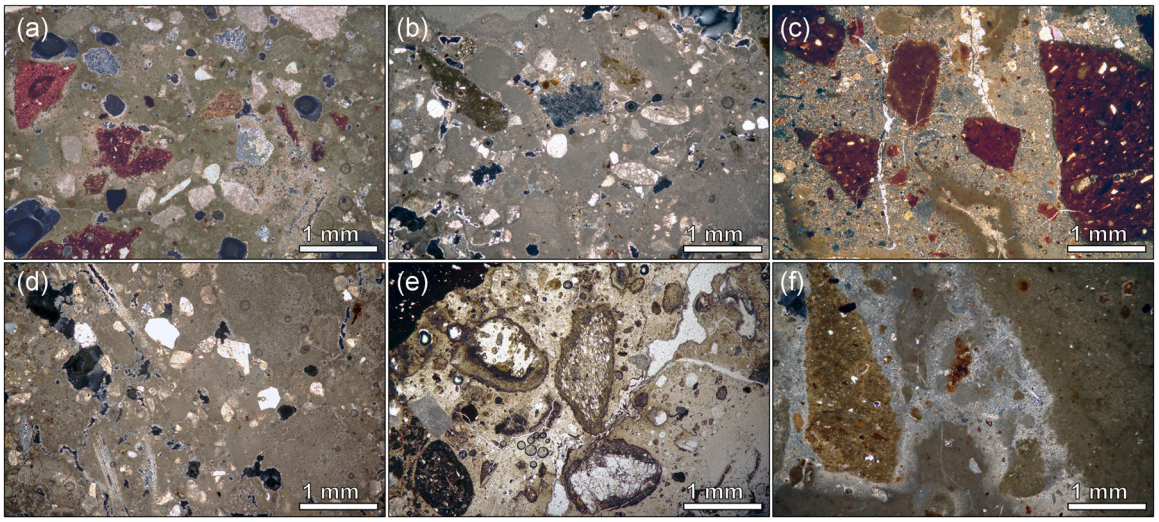

FIGURE 4 Optical microscopy micrographs of representative samples in polarized transmitted light (TL), crossed nicol (XN), or parallel nicol (PN). (a) WM_1 (Gr 1), TL-XN. The aggregate is represented by FF mixed with FS. (b) PREP_12 (Gr 1b), TL-XN. The aggregate is represented by sporadic FF mixed with prevalent FS. (c) CM_1 (Gr 2), TL-XN. The aggregate is composed of millimetric FF and finely ground FP. (d) PREP_1 (Gr 3), TL-XN. The aggregate is composed of prevalent carbonate sand and quartz (FS). Fibers of plants are present (top and bottom, sx). (e) VM_4 (Gr 4), TL-PN. At the center of the image, some submillimetric clasts of pyroclastic rocks, clearly edged by reaction rims. (f) PREP_5, TL-XN. The aggregate is composed of pluri-millimetric FF with a small amount of finely ground FP. FF, fired-clay fragments; FP, fired-clay powder [Color figure can be viewed at wileyonlinelibrary.com]

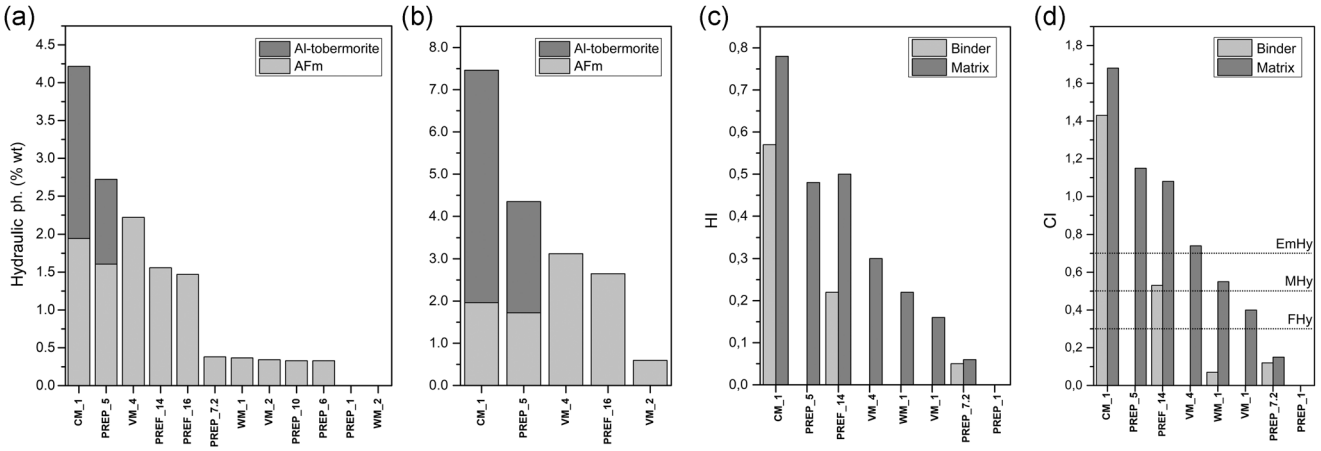

FIGURE 5 Distribution graphs of the samples in relation to their hydraulic properties, investigated by XRPD and SEM-EDS analyses. (a) Graph of crystalline hydraulic phases (AFm and Al-tobermorite), expressed in wt%, of a selection of representative samples after XRPD-bulk analysis; (b) graph of pozzolanic phases (AFm and Al-tobermorite), expressed in wt%, of a selection of representative samples after XRPD-binder analysis; (c) HI of selected samples in relation to the hydraulicity rates of binder (lime lumps) and matrix, determined according to Boynton (1966); and (d) CI of selected samples in relation to the hydraulicity rates of the binder (lime lumps) and the matrix, determined after Boynton (1966). The values represent the mean of multiple EDS semiquantitative measurements. EmHy, eminently hydraulic; FHy, feebly hydraulic; MHy, moderately hydraulic; SEM-EDS, scanning electron microscopy coupled with energy-dispersive spectroscopy; XRPD, X-ray powder diffraction

FS and RM (Figure 4b). For these samples, the B/A ratio is found to be around 0.8 or 0.9.

(2) Gr 2 samples are pinkish (2.5 YR 8/3), highly cohesive *cocciopesto* mortars, with a consistent occurrence of FF and diffused micrometric FP, closely mixed with the binder. The occurrence of FS is negligible (Figure 4c). The binder matrix has low birefringence colors, likely due to the diffused formation of hydrate products (Pecchioni et al., 2014). Lime lumps are minimal (2%), and the porosity is limited (4%–5%).

(3) Gr 3 samples are binder-rich lime mortars (B/A ratio 1.8 and 1.9). The presence of lime lumps is highly pronounced (16%–24%). The aggregates represent less than 35% of the samples and they are composed of subrounded medium to fine FS with a variable

sorting. Calcareous discarded *tesserae* chips, used as aggregates, have been recognized in sample PREP_1, where marble chips and straw were also detected (Figure 4d).

(4) Gr 4 samples are characterized by the presence of small subrounded clasts of volcanic lava and pumice. They are particularly abundant in VM_4, representing about the 12% of the sample (Figure 4e), while they are less in VM_1. The remaining aggregate's fraction is composed of FS and FF (with traces of FP). The binder matrix is inhomogeneous. The low birefringence colors detected in certain zones are probably indicative of the strong development of calcium alumino-silicate hydrates (Pecchioni et al., 2014).

(5) Some samples do not cluster within the outlined distribution: the first pair includes layers PREP_7.1 and 7.3, reported in Figure 3a. The former is made of homogeneous lime putty with the sporadic occurrence of FS, while the latter is made of a concrete rich in FS represented by medium to fine gravel (Wentworth, 1922), less frequent coarse FF, and sporadic volcanic rock clasts.

(6) The second pair of outliers is PREP_5 and PREP_6. The former is similar to Gr 2 mortars, as it presents an aggregate entirely composed of coarse FF, but the presence of FP is low (Figure 4f), and the SD of the aggregates is high (3.8). The binder matrix looks extremely zoned: areas characterized by low birefringence alternate with others having high birefringence. On the other hand, PREP_6 is characterized by an aggregate fraction predominantly represented by reused mortar fragments (RM, 37%), while both FF and FS represent minor aliquots.

5.2 | Hydraulic properties

The hydraulic properties of mortar samples were determined by coupling quantitative XRPD-*bulk* and *binder* analyses (Table S4) with punctual semiquantitative SEM-EDS investigations (Table S5).

For some mortars, XRPD-*bulk* analysis reported high aliquots of calcium (alumino)silicate hydrates C–(A)–S–H and calcium aluminate hydrates C–A–H, whose formation is determined by the pozzolanic interaction between the aerial lime paste with FF and, specifically, FP. Crystalline C–(A)–S–H is structured in the form of anthropogenic tobermorite 11 Å, also known as Al-tobermorite (Jackson et al., 2013, 2017). Crystalline C–A–H consists of AFm phases, in the form of hydrocalumite and hydrotalcite (Matschei et al., 2007). The sum of Al-tobermorite and AFm represents about 4.2 wt% of the bulk sample CM_1 (pool coating) and 2.7 wt% of PREP_5 (*opus sectile* bedding), respectively (Figure 5a). For both mortars, probably also a relevant fraction of the amorphous component could be related to gel-like C–(A)–S–H or C–A–H. The occurrence of brucite in sample CM_1 can be considered as a newly formed phase connected with the pozzolanic reaction of the material (Jackson et al., 2014; Vola et al., 2011). The absence of this phase in all other analyzed samples makes the calcination of dolomitic limestone (Bläuer-Böhm & Jagers, 1997) unlikely, as suggested also by the EDS investigations of highly calcic lime lumps. The presence of free magnesium ions in the system probably depends on de-dolomitization phenomena of dolomitic aggregates (Katayama, 2010) in a high-pH environment.

Samples from the S20 *opus caementicium* platform (PREF_14 and 16), as well as sample VM_4, are characterized by the relevant formation of crystalline AFm, but no Al-tobermorite was detected. In VM_4, anomalous high rates of aragonite (5.2 wt%) and vaterite (3.4 wt%) were found. The latter was also documented (2.5 wt%) in PREP_5. These phases represent metastable anthropogenic transitional products formed after decalcification and recarbonation of calcium carbonates along with the pozzolanic reaction of the material (Jackson et al., 2014, 2017; Morandeau et al., 2014; Thiery et al., 2007). Finally, the presence of 1.0 wt% phillipsite in VM_4 can be related to the authigenic zeolitization of volcanic aggregates (De'Gennaro et al., 1990, 2000).

Most of the remaining samples have feeble hydraulic properties, and only WM_2 and PREP_1 can be considered aerial compounds (no AFm phases are detected).

To properly describe and quantify the formation of the hydraulic phases, targeted XRPD-*binder* analyses were carried out on a limited selection of samples (Figure 6), which reported the same trend as that obtained from the XRPD-*bulk* analysis.

The formation of Al-tobermorite and AFm is still extremely evident in CM_1 (Al-tobermorite + AFm = 7.5 wt%) and in PREP_5 (Al-tobermorite + AFm = 4.3 wt%) (Figure 5b). Furthermore, the abundant amorphous fraction is likely related to the occurrence of gel-like C–(A)–S–H/C–A–H products. The high SiO_2 rates in the presence of Al_2O_3, reported in Figure 7a,b,b1,b2,

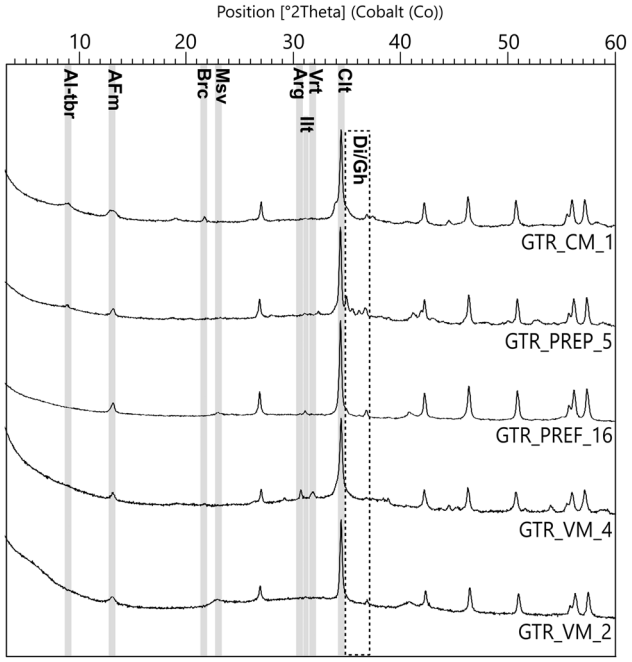

FIGURE 6 X-ray powder diffraction-*binder* spectra of representative samples with an indication of the principal phases. AFm, AFm phases; Al-tbr, Al-tobermorite; Arg, aragonite; Brc, brucite; Clt, calcite; Di, diopside; Gh, gehlenite; Ilt, Illite; Msv, muscovite; Vrt, vaterite

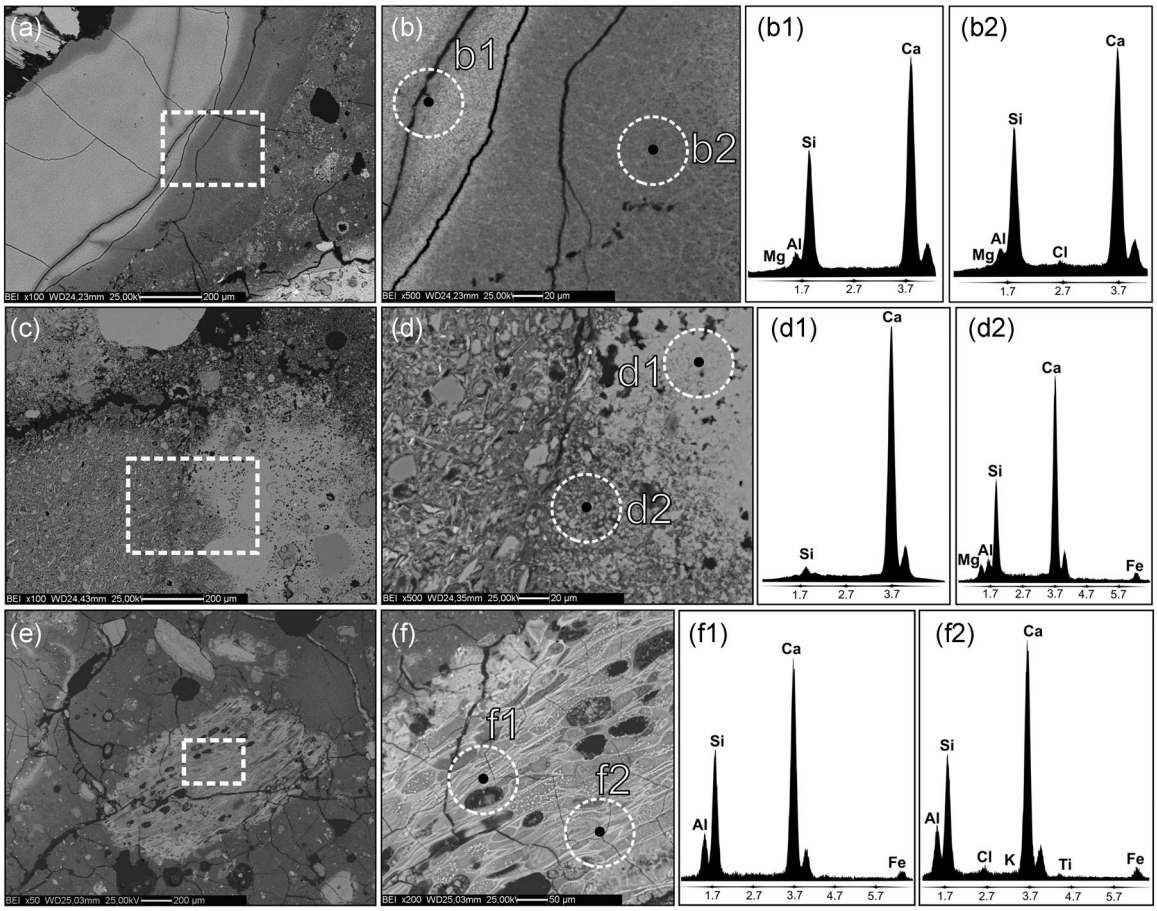

FIGURE 7 SEM-EDS analysis of representative samples. Backscattered electron acquisitions (BSE). (a) CM_1, unmixed lump of lime; (b) magnification of the dotted area in (a); (b1) EDS microanalysis of a point of the lime lump with high interference colors; (b2) EDS microanalysis of a point of the lime lump with low interference colors; (c) WM_1, binder matrix; (d) magnification of the dotted area in (c); (d1) EDS microanalysis of a point of the binder matrix with high interference colors; (d2) EDS microanalysis of a point of the binding matrix with low interference colors; (e) VM_4, pumice clast; and (f) magnification of the dotted area in (e): (f1) EDS microanalysis of a point of the core of the volcanic glass (altered) and (f2) EDS microanalysis of a point of the core the volcanic glass (altered). SEM-EDS, scanning electron microscopy coupled with energy-dispersive spectroscopy

demonstrate the formation of C–(A)–S–H in the outer perimeter of a lime lump in CM_1.

The remaining samples PREF_16, VM_2, and VM_4 are moderately hydraulic, as the formation of AFm is limited. XRPD-*binder* analysis detected the presence of hydroxyapophyllite (0.2 wt%) in VM_4: this is a silicate hydrate commonly associated with zeolites, whose formation is due to the pozzolanic interaction between calcium and potassic components of volcanic rocks (Rochelle et al., 2016).

SEM-EDS punctual analyses on the binder matrix confirmed XRPD investigations (Figure 5c,d).

The highest *HI* and *CI* (0.72 and 1.68), indicative of eminently hydraulic mixtures, were detected in sample CM_1. This confirms how the strong pozzolanic interaction between the micrometric fired-clay powder and the aerial lime contributes to the formation of calcium silicoaluminate hydrates (Coutelas et al., 2004; Lancaster, 2019; Teutonico et al., 2000). The high *HI* and *CI* are also found in sample PREF_14 (0.45 and 1.08, respectively). On the other hand, the chemical investigation of sample PREP_5 confirmed the zoning hypothesized after OM investigations: low birefringence areas are characterized by *HI* and *CI* of 1.11 and 2.57, respectively, while high birefringence areas have *HI* and *CI* of 0.15 and 0.41 (mean *HI* and *CI*: 0.48 and 1.15), respectively.

VM_1, VM_4, and WM_1 showed *HI* and CI between 0.16 and 0.31 and 0.40-0.74, indicative of moderately hydraulic mixtures. However, also in these cases, the matrix appears zoned, with eminently calcic carbonated areas surrounded by C–(A)–S–H/C–A–H-enriched zones with low birefringence (Figure 7c,d,d1,d2). For sample VM_4, the high *HI* and *CI* (0.31 and 0.74) could also depend on the strong interaction between lime and the reactive glassy fraction of the volcanic aggregates, acting as natural *pozzolans*. Most of these clasts altered and showed strong development of CaO-enriched fluids even in the inner cores (Figure 7e,f,f1,f2).

Finally, *HI* ≤ 0.06 and CI ≤ 0.15 of samples PREP_1 and PREP_7.2 indicate mixtures presenting low to null hydraulic properties.

5.3 | Provenance of raw materials

The majority of the raw materials used in the production of the mortar-based materials of the Great Baths were locally sourced. From a petro-mineralogical point of view, carbonate and silicate aggregates are fully compatible with the sediments of the Isonzo–Natisone–Torre fluvial network. These are characterized by a dominant component of calcareous/dolomitic sands and gravels, with a secondary presence of chert and quartz sands (Gazzi et al., 1973; Marocco, 2009).

Less is known about the carbonate rocks used for the production of lime. SEM-EDS analyses were performed on lime lumps of some samples (WM_1; PREP_1, 7.2, 14; CM_1). In most cases, for samples with pronounced hydraulic properties, we observed an intense development of gel-like C–(A)–S–H in the micropores of lime lumps. This indicated a clear alteration of the original geochemical profile of the binder. Only in PREP_1 and WM_1 did the analyzed lime lumps yield high CaO and low MgO contents, suggesting the calcination of almost pure calcic limestones (Zacharopoulou, 2009). This profile is compatible with the geochemistry of the limestones locally outcropping in the Isontine and Triestine Karst (G. B. Carulli & Onofri, 1960; Cucchi et al., 2015; Cucchi & Gerdol, 1985; Tentor et al., 1994) as well as in Istria (Lazzarini, 2006).

The provenance of the three volcanic vaulting lightweight caementa and aggregates detected in VM_1 and VM_4 samples was also determined. These rocks were surely imported in Aquileia, as no volcanic districts are present nearby, as the region is dominated by limestone and dolostone outcrops (G. Carulli, 2006). OM and XRPD investigations on *caementa* samples were performed for a preliminary determination of their provenance. XRPD data have been recalculated at 100% after the removal of binder-related phases, that is, calcite (Table S6).

VM_1_G is a yellowish (2.5 Y 8/4), highly vesicular pyroclastic pumice (Figure 8a1). Its texture is glassy (Figure 8a2). The rare phenocrysts are represented by biotite, Ca-plagioclases (bytownite/anorthite), K-feldspars (sanidine), and sporadic augite. The quartz content is extremely low (0.9 wt%). The zeolitization products are extremely pronounced: 48.3 wt % phillipsite and 1.9 chabazite. Percentages have been normalized at 100% after the removal of calcite (31.7 wt%) and vaterite (0.6 wt%). These latter phases are related to the neoformation of CaO-based metastable products into the voids of the rock, along with the pervasive

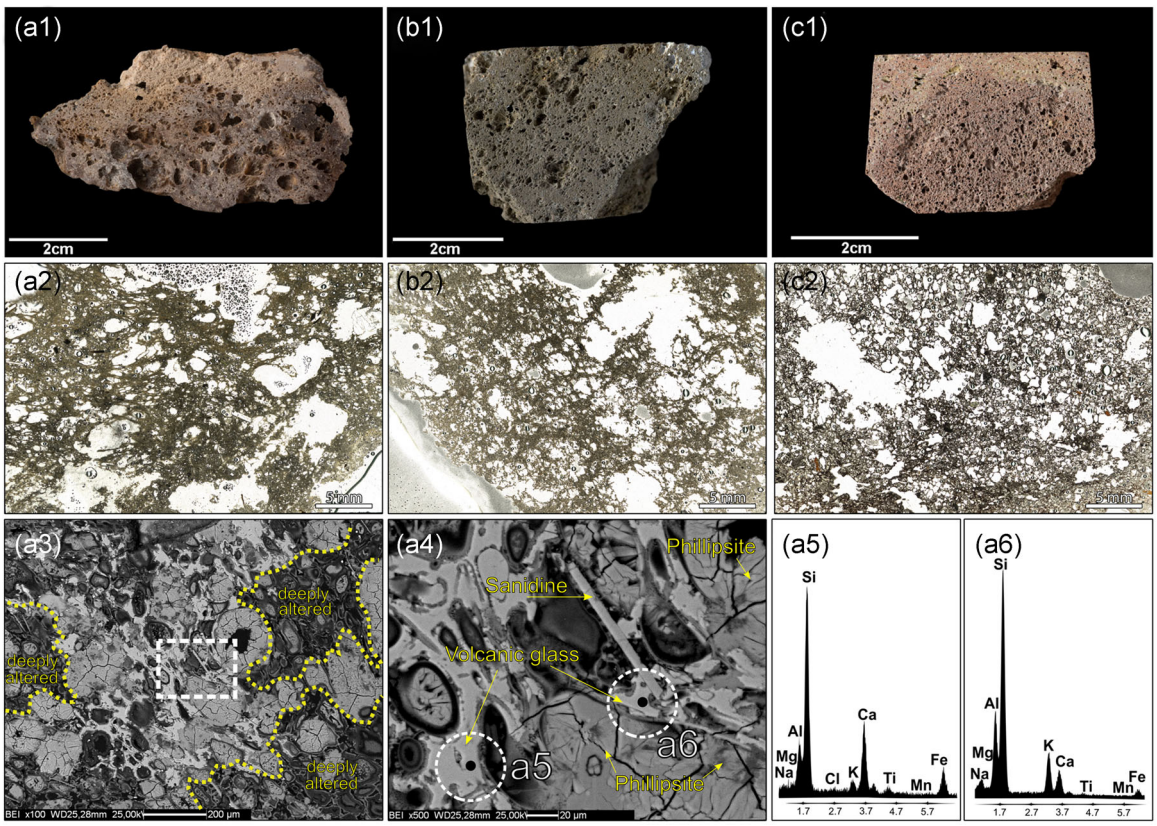

FIGURE 8 Upper band: the three sampled lightweight *caementa* after petrographic cut: (a1) VM_1_G; (b1) VM_1_N; and (c1) VM_4_R. Middle band: optical microscopy acquisitions in polarized transmitted light (TL) of lightweight *caementa* samples in parallel nicol (PN): (a2) VM_1_G; (b2) VM_1_N; and (c2) VM_4_R. Lower band: SEM-EDS analysis of sample VM_1_G, backscattered electron acquisitions (BSE): (a3) core of the samples VM_1_G, deeply altered by a pozzolanic reaction (low interference colors); (a4) magnification of the dotted area in (a3); (a5) EDS microanalysis of a feebly altered point of pumice glass; and (a6) EDS microanalysis of an unaltered point of the pumice glass. SEM-EDS, scanning electron microscopy coupled with energy-dispersive spectroscopy [Color figure can be viewed at wileyonlinelibrary.com]

pozzolanic reaction of the material, as revealed through SEM-EDS investigations of the sample (Figure 8a3–a6).

VM_1_N is a vesicular grayish-brown (2.5 Y 5/2) pumiceous scoria (Figure 8b1,b2), rich in K-feldspar (sanidine–anorthoclase) microlites (56.4 wt%), associated with Ca-plagioclases of the anorthite–bytownite type (11.0 wt%). Augitic phenocrysts are more frequent than biotite ones. The glassy fraction is low in comparison with sample VM_1_G (13.0 wt%), as well as phillipsite (11.9 wt%). On the other hand, the percentage of quartz is higher (3.2 wt%).

VM_4_R is a highly vesicular tephritic lava (Figure 8c1) with a porphyritic–hyalopilitic texture (Figure 8c2). The groundmass is predominantly made of k-feldspars of sanidine (46.4 wt%) and subordinated Ca-plagioclases (17.3 wt%). Phenocrysts of augite are frequent (8.2 wt%). The presence of zeolites is feeble (phillipsite 1.0 wt %, chabazite 0.2 wt%). The dark-red color of the sample (2.5 YR 6/4) depends on the concentration of hematite (6.0 wt%).

The sanidine, documented in all samples and especially in VM_1_N, is a recurrent mineral in the vulcanism of the Roman Comagmatic region (Marra et al., 2013; Peccerillo, 2005). The presence of authigenic phillipsite, which is particularly abundant in samples VM_1_G and VM_1_N, is common in the Phlegrean products of the NYT formations (De'Gennaro et al., 1990, 2000). This zeolite is frequently documented in Roman mortars and concretes containing Phlegrean pyroclasts (Jackson et al., 2014; Rispoli et al., 2019, 2020; Stanislao et al., 2011; Vola et al., 2011).

On the other hand, textural and petro-mineralogical features of sample VM_4_R are fully compatible with the Vesuvian "foam lava" (Cinque & Irollo, 2004; Di Girolamo, 1968; Marra et al., 2013), a porous lava pillow formation of the Somma-Vesuvius eruptive unit (Langella et al., 2009; Santacroce, 1987).

Geochemical analyses performed through XRF provided a better definition of the provenance of the three samples (Table S7).

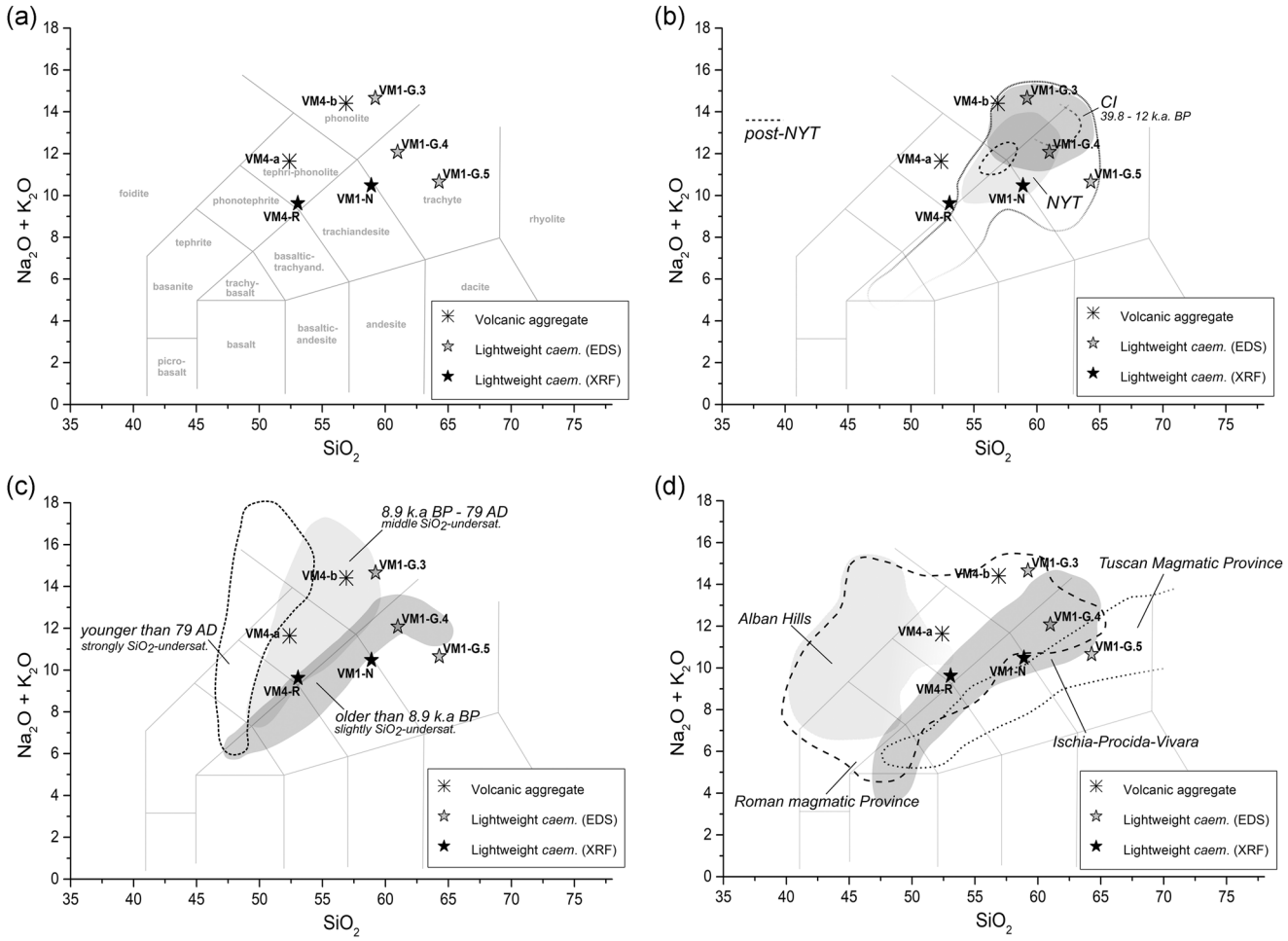

FIGURE 9 TAS scatterplots of the clast of lightweight *caementa* and volcanic aggregates of the vaults. (a) Sample distribution in relation to volcanic rocks' chemistry (after Le Bas et al., 1986); (b) sample distribution in relation to the Phlegrean fields areas of the Campanian Ignimbrite (CI), Neapolitan Yellow Tuff (NYT), and post-NYT events (data from Marra, Anzidei, et al., 2016; Morra et al., 2010; Peccerillo, 2005); (c) sample distribution in relation to the three main eruptive facies of the Vesuvian products' fields (data from Morra et al., 2010; Peccerillo, 2005); and (d) sample distribution in relation to the fields occupied by the products of the Roman magmatic province, Tuscan Magmatic province, and Ischia-Procida-Vivara's volcanoes (data from Avanzinelli et al., 2009; Boari et al., 2009; Marra et al., 2009; Peccerillo, 2005). TAS, total alkali silica

All the *caementa* samples plot in the total alkali silica (TAS) fields (Le Bas et al., 1986) occupied by the slightly - middle SiO_2 undersaturated volcanic rocks (Figure 9a).

VM_1_N falls in a trachyandesite field compatible with the area of the Phlegrean vulcanism (Morra et al., 2010; Peccerillo, 2005) (Figure 9b). It shows good overlap with some products of the NYT or later volcanic activities (12–8.4 and <8.4 k.a. B.P.) (Marra, Anzidei, et al., 2016).

VM_4_R, on the other hand, plots in between the Somma-Vesuvius products older than 8.9 k.a. B.P. and those younger than 79 AD (Peccerillo, 2005; Santacroce et al., 2008) (Figure 9c).

Finally, VM_1_G returns anomalous low values of alkali and silica. The surprisingly high content of CaO demonstrates the deep development of C–(A)–S–H and CaO-enriched fluids in the sample, as suggested by the results of the XRPD analysis too. The high loss of ignition (LOI) of the sample (19.2) confirms this assumption. Both VM_1_N and VM_4_G samples have a > 3.0 (4.1 and 3.5, respectively), which is indicative of a slight alteration too (Lancaster et al., 2011; Marra et al., 2013). This aspect does not make XRF major elements suitable for an in-depth provenance analysis.

To acquire a better major chemical element profile for VM_1_G, we performed six punctual SEM-EDS investigations on three areas of the volcanic glass that appeared unaltered. The mean values for each zone of the sample under investigation are reported in Table S8. In the TAS, they cover a wide area ranging from the trachyte's to the phonolite's fields (Figure 9a). Also, in

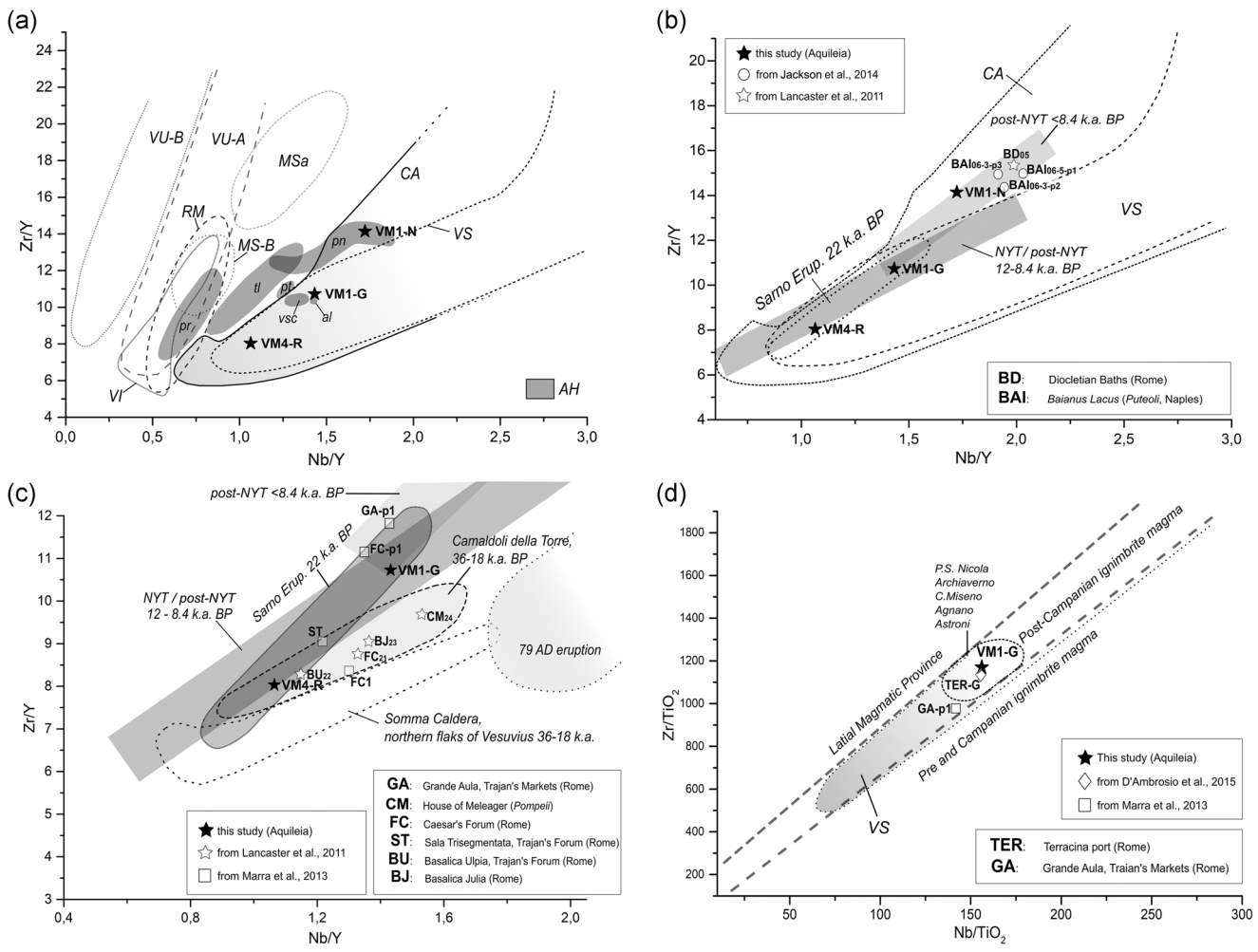

FIGURE 10 Trace element scatterplots of the lightweight *caementa* samples of the vaults. (a) Nb/Y versus Zr/Y scatterplot of *caementa* samples in relation to the fields occupied by volcanic products of the Latian, Tuscan, and Campanian magmatic provinces (modified after Marra & D'Ambrosio, 2013; Marra et al., 2013); (b) Nb/Y versus Zr/Y graph of the *caementa* samples in relation to the fields occupied by volcanic products of the Campanian magmatic province (modified after Marra et al., 2013); (c) Nb/Y versus Zr/Y scatterplot of the *caementa* samples in relation to the fields occupied by volcanic products of the Phlegrean and Vesuvian magmatic units (modified after Marra et al., 2013); and (d) Nb/TiO_2 versus Zr/TiO_2 scatterplot of the *caementa* samples in relation to the geological fields occupied by volcanic products of the Campanian, Phlegrean, and Vesuvian magmatic units (modified after D'Ambrosio et al., 2015; Marra et al., 2013). AH, Alban Hills and subunits; al, Alban Crater; CA, Campanian volcanic district; MSa/MS-B, Mounts Sabatini district (Lazio); pn, "Pozzolane Nere"; pr, "Pozzolane Rosse"; pt, "Pisolitic tuff"; RM, Roccamonfina volcano (Campania); tl, "Lionato tuff"; VI, Vico volcanic district (Lazio); VS, Vesuvian volcanic district; vsc, Villa Senni eruptive unit; VU-A/VU-B, volcanic district of Vulsinii (Lazio)

this case, therefore, SEM data cannot be considered as conclusive. Also, the geochemical profile of the *caementa* reported in the TAS cannot be considered as indicative of a specific volcanic district. In fact, as shown in Figure 9d, good matches can also be traced with certain products of Ischia-Procida's and Roccamonfina's volcanoes of the Campanian district (Peccerillo, 2005), as well as with some products of the Latial and Tuscan Magmatic Province (Avanzinelli et al., 2009; Boari et al., 2009). Nevertheless, all the samples do not match with the ultrapotassic products of the Alban Hills (Boari et al., 2009; Marra et al., 2009; Peccerillo, 2005).

Considering the high variability of the TAS, the analyses of Zr/Y versus Nb/Y and Nb/TiO_2 versus Zr/TiO_2 were crucial to confirm the exact provenance of the *caementa* (Brandon et al., 2014; D'Ambrosio et al., 2015; Jackson et al., 2013; Lancaster et al., 2011; Marra & D'Ambrosio, 2013; Marra et al., 2009, 2011, 2013; Marra, Anzidei, et al., 2016; Marra, D'Ambrosio, et al., 2016). Nonetheless, it cannot be totally excluded that the alteration of the volcanic glass, in particular, for VM_1_G, could have led to the depletion of some trace elements too.

VM_1_N presents high ratios of Zr/Y and Nb/Y (Figure 10a). This sample is fully compatible with volcanic products of Campania, but it also matches some pyroclastic deposits of the so-called "Pozzolane Nere" of the Alban Hills (D'Ambrosio et al., 2015; Jackson et al., 2007; Marra et al., 2009). However, the ultrapotassic composition of the Alban Hills' products is incompatible with the chemical composition of VM_1_N, as revealed by the TAS diagram, confirming its Campanian provenance.

The ratios of Zr/Y and Nb/Y in samples VM_1_N are close to those reported in some archaeological samples taken from the vaults of the Baths of Diocletian in Rome (Baths of Diocletian 05), analyzed in Lancaster et al. (2011) and Marra et al. (2013) (Figure 10b). This profile is also compatible with the pale grayish-orange pumice specimens from the *opus caementicium* piers of *Portus Baianus* (BAI.06.03.P2; BAI.06.05b.P1; BAI.2006.03.P3), analyzed in the framework of the ROMACONS project (Jackson et al., 2013, 2014), which were ascribed to the most recent Phlegraean eruptions (post-NYT <8.4 k.a. B.P.).

Based on the Nb/Y versus Zr/Y distribution, VM_1_G falls in an overlapped zone occupied by volcanic products of NYT and post-NYT activities (12–8.4 and <8.4 k.a. B.P.) (Figure 10b). It also partially overlays the area occupied by the Vesuvian products of the Sarno eruption (22 k.a. B.P.), the so-called "Pomici di Base" (Santacroce et al., 2008), and it feebly matches some products of Ischia and Procida's volcanoes (Marra et al., 2013). VM_1_G correlates with a volcanic rock specimen collected from the vaults of the *tabenae* of the Forum of Caesar in Rome (FC-p1), for which it was not possible to pinpoint the origin among the Phlegrean, Ischia-Procida, or Vesuvian areas (Marra et al., 2013) (Figure 10c). A second similar pumice sample comes from the vaults of the Great Hall of the Markets of Trajan (GA-p1), whose provenance, suspected Vesuvian (Marra et al., 2013), has been later related to Sarno 22 k.a. B.P. products, as revealed by the Zr/TiO_2 vs Nb/TiO_2 plot (D'Ambrosio et al., 2015).

Therefore, the information obtained by Nb/Y versus Zr/Y does not further restrict the provenance of VM_1_G. Based on the Zr/TiO_2 versus Nb/TiO_2 plot (Figure 10d), it closely resembles a sample taken from the harbor piers of Terracina (TER-G), which has been associated with post-NYT products (D'Ambrosio et al., 2015; Marra, Anzidei, et al., 2016). The Zr/TiO_2 versus Nb/TiO_2 plot can be considered reliable, as TiO_2 appears to be more stable than Y, even after HCl attack (D'Ambrosio et al., 2015). Therefore, the provenance of sample VM_1_G is surely Campania, while a stronger correlation with the post-NYT products may be tracked only on the basis of the Zr/TiO_2 versus Nb/TiO_2 plot.

Finally, as outlined before, sample VM_4_R presents the peculiar petro-mineralogical and textural features of the Vesuvian lava pillows. In the TAS diagram, it overlaps the Vesuvian products. In the Nb/Y versus Zr/Y plot (Figure 10b), it falls within the Somma-Vesuvius field, overlapping the area of the Sarno eruption (22 k.a. B.P.) (Marra et al., 2013) as well as that of the lava flows dated 36–18 k.a. B.P. and documented with a deep borehole in the southern flank of Somma-Vesuvius (Di Renzo et al., 2007). It also slightly overlaps the NYT field, but considering the TAS diagram as well as its petro-mineralogical features, it is not compatible with the low SiO_2-undersatured products of NYT activity. In detail (Figure 10c), the Nb/Y versus Zr/Y profile of VM_4_R matches with that of some lava samples taken from the vaults of a series of Imperial buildings in Rome (Basilica Ulpia 022, Forum of Caesar 021, Basilica Iulia 023), analyzed in Lancaster et al. (2011). These were attributed by Marra et al. (2013) to the Somma-Vesuvius lavas cropping on the southern flanks of the volcano (36–18 k.a. B.P.).

Combining OM, XRPD, SEM-EDS, and XRF analyses, the provenance of the three lightweight caementa was defined. VM_1_G and VM_1_N came from the Phlegrean volcanic units of the post-NYT activity (i.e., Astroni, Agnano, Archiaverno, and Miseno units), cropping around *Puteoli*. Nevertheless, the Vesuvian provenance of sample VM_1_G cannot be completely excluded. VM_4_R, on the other hand, can be safely assigned to Vesuvian lava formations older than 8.9 k.a. B.P.

The origin of volcanic clasts used as aggregate is barely determinable, as they are usually altered due to the pozzolanic reaction. The unaltered glassy portions of two volcanic aggregates in sample VM_4, labeled VM_4-a and VM_4-b, was detected and analyzed by SEM-EDS (Table S8). In the TAS (Figure 9a), they fall roughly in the same fields occupied by the lightweight *caementa*, but the exact sourcing area can differ.

Sporadic clasts of volcanic rocks have also been documented in layers PREP_7.2 and 7.3. Their presence is probably accidental. No provenance analyses have been performed for the volcanic rocks in these samples.

6 | DISCUSSION

The analysis of the samples collected from the site of the Great Baths proved to be extremely important within the framework of the archaeological research carried out in Aquileia.

The distribution of the samples in the groups is in agreement with the structural use of the mortars: those collected from the vaults

in *opus caementicium* (Gr 4) can be distinguished from those referring to hydraulic infrastructures (Gr 2). Both these groups differ from the most populated one, represented by the samples coming from floor bedding layers and wall joints (Gr 1). The chronology of production does not particularly bias the composition of the samples, but it must be highlighted that Gr 3 comprises only mortars related to phases later than Ia.

The outstanding quality of the mortar-based materials of the complex is highlighted by the hydraulic properties of most of the samples. An experienced chain of production can be perceived in the slight differences in composition and hydraulic characteristics of the samples, which depend on the structural use: joint mortars and bedding mixtures for some types of floors (i.e., mosaics) are quite ordinary; on the other hand, the manufacture of mortars applied in critical structural units, such as hydraulic infrastructures and roofing systems, required the proper choice of raw materials and correct preparation of the mixture. This degree of "mixing care" has been parametrized by comparing samples according to their hydraulic properties, and quantifying the formation of calcium silicoaluminate hydrates through XRPD and SEM-EDS investigations.

The best mortars are the pool coatings that guarantee excellent waterproofing. XRPD data of sample CM_1 report a hydraulic rate three to five times higher than that of the *cocciopesto* mortars used in all the other water tanks of Aquileia (Dilaria, 2020). This trend does not change if we compare the *HI/CI* of CM_1 with that of cisterns' coating mortars from other Roman sites (De Luca et al., 2015; Miriello et al., 2018; Rispoli et al., 2019, 2020; Secco et al., 2020).

Further distinctions exist in "recipes" for pavements' bedding mortars according to the floor type. Good hydraulic properties have been reported for the sole sample PREP_5, coming from the substrate of the *opus sectile* pavement of the *frigidarium*. This is a common feature of the *opus sectile* pavements of Aquileia (Dilaria et al., 2016; Secco et al., 2018). Hydraulic compounds produced along with the pozzolanic reaction ensure waterproofing and strengthening of the material (Navrátilová & Rovnaníková, 2016, with references therein) to adequately support the heavy stone slabs of the revetment.

Mosaics' bedding mortars differ from the *opus sectile* ones. In most cases, mosaics were set on a single layer of *cocciopesto* with low hydraulic properties, while only in one case (PREP_7) was the pavement placed over a bedding distributed in up to three different layers, in agreement with the Vitruvian standard (Vitr. VII, 1, 1–7): a 3.5–5.0 cm thick *cocciopesto* layer (*nucleus*) (layer PREP_7.2) and an inner concrete *stratum* with gravel and FFs, about 7.0–8.5 cm thick (*rudus*) (layer PREP_7.3), are placed over a layer of loose stones, FFs, and marble chips (*statumen*). Above the screed, *tesserae* were set on a thin lime putty film (Dunbabin, 1999; Moore, 1968, pp. 281–288), represented by the layer PREP_7.1. This is the typical Roman mosaic-making technique, which was usually adopted in the Republican and High Imperial Age. On the other hand, during the Late Imperial Age, the mosaics in Aquileia were set on shoddy beddings made of a single layer of friable sandy lime mortar laid over earthen dumps (Dilaria, 2020; Dilaria et al., 2016; Secco et al., 2018). The adoption of this weak making method can be recognized in the making of Phase Ib and Ic mosaics of the northern sector of the Great Baths, which were placed over mortars of the Gr 3. This demonstrates that the restorations of the complex were carried out by artisans with a lower level of experience than those who were working in the original building phase.

Samples PREF_14 and 16, collected from the S20 platform, are characterized by moderate hydraulic properties. Good impermeabilization was necessary for this structure, equipped with an sophisticated system of tanks and pools (Rubinich, 2020). The slight compositional differences among S20 samples (PREF_14, 15, and 16), observed via OM, are probably due to the width and depth of the platform, whose construction required a long time for completion. These nuances in the composition could reflect the daily preparation of mixtures (Coutelas, 2012). Similar considerations can be outlined for samples PREP_10 and 11 too, coming from different areas of a Phase Ib mosaic. On the other hand, the different composition and the abundant presence of RM in the sample PREP_6, which were not detected in PREP_5, could testify to important (undated) restoration of the SW portion of the pavement of the *frigidarium*.

The vaulting system of the baths is also sophisticated as demonstrated by the use of lightweight *opus caementicium*. The abundant presence of pluri-centimetric porous *caementa* testifies to a huge supply of material from the Gulf of Naples. Although no mention is reported in Latin treaties, the use of lightweight pumices, lava, or tuffs in the *opus caementicium* vaults of Roman monumental buildings has been archaeologically proven since the mid-1st century B.C., becoming established by the early 2nd century AD (Lancaster, 2005, pp. 59–64; Lancaster, 2011; Lancaster, 2015, pp. 29–38; Lancaster et al., 2011). A finer fraction of these volcanic rocks constitutes the aggregates of some mortars, but connecting this use to the Vitruvian concept of *pozzolana* (see section 1) may be incorrect. Their use was primarily intended for providing further light-weight properties to the vaults, as supposed by Bianchi et al. (2011), Jackson et al. (2010), Jackson, Logan, et al. (2011), who interpreted, in this way, analogous evidence from vaults of monuments in Rome. Furthermore, the hydraulic properties surely increase the strength of the *opus caementicium* structure exposed to major mechanical stress. The higher amount of porous volcanic aggregates in sample VM_4 in comparison with VM_1 may indicate the progressive lightening of the *opus caementicium* castings at higher elevations. This was a well-known practice in Roman times, with a famous example represented by the Pantheon (Lancaster, 2005, p. 62). Therefore, VM_4 might come from the uppermost portion of a vault, which was supposed to have higher light-weighting capabilities.

Considering the dating of the Great Baths, the use of imported rocks as vaulting *caementa* is one of the latest attestations of this tradition in the Roman Empire. The presence of Phlegrean pumices in the vaults of the *Thermae* of Diocletian in Rome (see paragraph 5.3),

whose construction, dated between 296 and 308 AD, was concluded a few decades before that of the baths of Aquileia, demonstrates that the exportation of these raw materials from Campania lasted during the Late Imperial Age, even though this trading network in the Mediterranean reached its climax a couple of centuries before (Hohlfeder & Oleson, 2014).

Another recurring aspect in Roman public buildings is the combined use of vaulting lightweight *caementa* quarried from different zones (Bianchi et al., 2011; Marra et al., 2013). This could be related to the different supplies of raw materials as the construction progresses, but it could also depend on the specific plan for gradually reducing the weight of the vaults at different heights using different materials (Marra et al., 2013).

Lancaster (2006, 2011) and Lancaster et al. (2011) suggested a shift in time in the sorting of the lightweight *caementa* in the vaulted buildings of Rome: while Vesuvian lavas were imported until the late 3rd century AD, the use of volcanic rocks other than the Vesuvian ones was prevalent in later ages. This hypothesis, which has been dubiously linked to a decline in land transport from Vesuvian quarries after the economic crisis of the 3rd century, is in contrast with the data from Aquileia here discussed.

However, the import of lightweight materials for vaulting structures was uncommon in Northern Italy in Roman times, even if the terms of comparison are very few. In fact, since the Middle Ages, most of the buildings in this region underwent marked spoliation of the construction materials and the roofing systems have been preserved only in a few cases. In the Villa of Sirmione (Garda Lake), dated to the Augustan-Tiberian Age, and in the *Capitolium* of Verona, lightweight *caementa* consist of local travertine or sandstones (Buonopane, 1987; Roffia et al., 2009, pp. 188–189), with negligible light-weighting capacity. The high costs for stone transport may have prompted the choice for locally supplied stones even if less efficient for weight reduction (Russell, 2013, pp. 141–200). Vaulting *caementa* in the Bath of Villeneuve in Frejus are surely imported as they are incompatible with the lithologies of the Massif Central of southern France (Excoffon & Dubar, 2011), but their provenance has not been verified.

The proximity to seaside or fluvial networks and to adequately equipped ports is an important factor affecting the trade of building stones other than marbles and decorative lithotypes (Russell, 2013, pp. 95–140). As far as Aquileia is concerned, the imported rocks could have been shipped from the harbors of *Puteoli*, Baia, and Miseno (Gianfrotta, 1998) to the river docks of Aquileia or, considering the late dating of the Baths, to the seaport of the neighboring Grado (Rebecchi, 1980). However, the maritime route from Campania to the northern Adriatic Sea is not straightforward, and the Gulf of Naples does not represent the closest area to Aquileia for the procurement of lightweight *caementa*. In the vaults of the Palace of Diocletian in Split (Croatia), Lancaster (2015, p. 33), reports the use of locally mined porous calcareous tufa, known as *sedra*. This reference demonstrates that near quarries for the provisioning of lightweight stones were still active in the 4th century AD and easily reachable by sea.

The choice for the supply of the materials from the Gulf of Naples has some alternative explanations: (a) the centuries-old knowledge of the prominent light-weighting capabilities of the Campanian porous rocks, which were largely used in the concrete vaulted buildings of Rome (Lancaster, 2011, 2015; Lancaster et al., 2011; Marra et al., 2013); (b) the provenance of the committee or craftmanship from central-southern Italy; (c) and the little diffusion of regional building materials, as the *sedra* calcareous tufa, out of the territories in which they were used.

Besides the use of porous *caementa* for *opus caementicium*, a finer fraction of the volcanic rocks from Campania was used as pozzolanic aggregate of vaulting mortars too. The trade of *pozzolans* from southern Italy to the north has been proven in other circumstances so far. The mention of the presence of Phlegrean pumices in the mortars of the harbor piers and vaults of the baths of *Forum Iulii* (Frejus) (Excoffon & Dubar, 2011), as well as in the joint mortars of the 3rd-century B.C. urban walls of Ravenna (Costa et al., 2001), was not validated by conclusive analysis. As recently discussed by Dilaria et al. (2019) and Dilaria (2020), pumices from *Campi Flegrei* are not even present in a concrete block in the foundations of the Republican urban walls of Aquileia (Bonetto et al., 2016) as, in this case, hydraulic properties were provided by a sort of natural hydraulic binder derived from the calcination of cherty limestones (Dilaria, 2020; Dilaria et al., 2019). The unique term of comparison on the use of pyroclastic rocks in *Cisalpina*, as *pozzolan* in stricto sensu, comes from the *opus caementicium* foundation of the *orchestra* (Dilaria, personal observation) of the theater of Aquileia (Ghiotto et al., 2021). Ongoing analysis will be focused on determining their exact provenance.

7 | CONCLUSIONS

In this study, we outline how decisive the analysis of ancient mortars is to solve traditional archaeological questions, such as the trading of raw materials and the technical expertise of crafts in antiquity. The data reported in this paper are rooted in the interrelationship between archaeology and geosciences and are focused on the understanding of archaeological sites and ancient socioeconomic relations through the investigation of geomaterials such as mortar-based ones.

Adopting this multidisciplinary approach, we are now able to fill the gap, re-evaluating the towns of ancient *Cisalpina* no longer as peripheral entities of the Empire, but rather as deeply rooted in the technical awareness of the Roman tradition. In fact, the full outcomes of the research demonstrate how remarkable the financial effort for the construction of the Great Baths was: only a high-ranked committee, such as the Constantinian imperial family, could have guaranteed the best workmanship and building materials available on the market at the time. No other public or private building in Aquileia achieved the same high-quality standard as far as mortar-based materials are concerned (Dilaria, 2020). Besides, the superb manufacture of mosaic decorations, which are considered a driving model for the Late Imperial iconography of Aquileia and, in a broader sense, *Cisalpina* (Novello, 2017), confirms the outstanding features of the building.

Finally, the late dating of the Great Baths provides new scenarios about the transfer of artisans and materials from the center to the north

of the peninsula during the Late Imperial Age, which requires further analysis. It is well known that the beginning of the 4th century represented for the main towns of Northern Italy (Aquileia, Ravenna, and *Mediolanum* in particular) a period of remarkable development and sociopolitical centrality. As stated by Ausonius, Aquileia became one of the largest cities of the Roman Empire, and the Great Baths can be considered one of the best examples of the constructive impulse of the time.

Unfortunately, the constructive *floruit* of the early 4th century ended quickly. The limited care devoted to the making of bedding mortars of the mosaics of the northern sectors in phases Ib and, in particular, Ic, indicates that the great achievement represented by the construction of the Great Baths was almost completely depleted by the end of the century.

ACKNOWLEDGMENT

Francesca Andolfo is gratefully acknowledged for revising the English text. Open Access Funding provided by Universita degli Studi di Padova within the CRUI-CARE Agreement.

AUTHOR CONTRIBUTIONS

Simone Dilaria, Jacopo Bonetto, and Michele Secco designed the research; Gilberto Artioli and Jacopo Bonetto supervised the research project; Simone Dilaria and Marina Rubinich performed the samplings; Simone Dilaria and Michele Secco performed the sample preparation; Simone Dilaria, Michele Secco, Domenico Miriello, and Donatella Barca analyzed the samples; Simone Dilaria, Jacopo Bonetto, Marina Rubinich, and Michele Secco interpreted the archeometric results; Simone Dilaria drafted Sections 1, 3, 4.1, 5, 6, and 7; Marina Rubinich drafted Section 2; Michele Secco drafted Sections 4.2 and 4.3; and Domenico Miriello drafted Section 4.4. All authors collaborated in the revision of the manuscript.

ORCID

Simone Dilaria http://orcid.org/0000-0001-6296-3388
Michele Secco https://orcid.org/0000-0002-9293-0189
Marina Rubinich https://orcid.org/0000-0003-3324-4143
Jacopo Bonetto https://orcid.org/0000-0001-6015-9898
Domenico Miriello https://orcid.org/0000-0003-4647-6947
Donatella Barca https://orcid.org/0000-0002-3087-8418
Gilberto Artioli https://orcid.org/0000-0002-8693-7392

REFERENCES

Addis, A., Secco, M., Marzaioli, F., Artioli, G., Chavarria Arnau, A., Passariello, I., Terrasi, F., & Brogiolo, G. P. (2019). Selecting the most reliable ^{14}C dating material inside mortars: The origin of the Padua cathedral. *Radiocarbon*, *61*(2), 375–393. https://doi.org/10.1017/RDC.2018.147

Alonso-Olazabal, A., Ortega, L. A., Zuluaga, M. C., Ponce-Antón, G., Jiménez Echevarría, J., & Alonso Fernández, C. (2020). Compositional characterization and chronology of Roman mortars from the archaeological site of Arroyo De La Dehesa De Velasco (Burgo De Osma - Ciudad De Osma, Soria, Spain). *Minerals*, *10*, 393. https://doi.org/10.3390/min10050393

Appolonia, L., Vaudan, D., & Glarey, A. (2010). Lo studio delle malte del Teatro romano di Aosta: una ricerca in corso. *Bollettino della Soprintendenza per i Beni Culturali della Valle D'Aosta*, *6/2009*, 249–252.

Avanzinelli, R., Lustrino, M., Mattei, M., Melluso, L., & Conticelli, S. (2009). Potassic and ultrapotassic magmatism in the circum-Tyrrhenian region: Significance of carbonated pelitic vs. pelitic sediment recycling at destructive plate margins. *Lithos*, *113*(1–2), 213–227. https://doi.org/10.1016/j.lithos.2009.03.029

Baccelle Scudeler, L., & De Vecchi, G. (2003). Tessitura e composizione degli aggregati presenti nella malta dell'*opus caementicium* nell'anfiteatro romano di Padova. In G. Tosi (Ed.), *Gli edifici per spettacoli nell'Italia romana I* (pp. 961–968). Quasar.

Belfiore, C. M., Fichera, G. V., La Russa, M. F., Pezzino, A., Ruffolo, S. A., Galli, G., & Barca, D. (2014). A multidisciplinary approach for the archaeometric study of pozzolanic aggregate in Roman mortars: The case of Villa dei Quintili (Rome, Italy). *Archaeometry*, *57*(2), 269–296. https://doi.org/10.1111/arcm.12085

Bianchi, E., Brune, P., Jackson, M., Marra, F., & Meneghini, R. (2011). Archaeological, structural, and compositional observation of the concrete architecture of the Basilica Ulpia and Trajan's Forum. In Å. Ringbom & R. L. Hohlfelder (Eds.), *Building Roma Aeterna: Current research on Roman mortar and concrete, Proceedings of the Conference, Helsinki, 27-29/03/2008, Commentationes Humanarum Litterarum* (Vol. 128, pp. 73–95). Publication of the Societas Scientiarum Fennica.

Bläuer-Böhm, C., & Jägers, E. (1997). Analysis and recognition of dolomitic lime mortars. In H. Bearat, M. Fuchs, M. Maggetti, & D. Paunier (Eds.), *Roman wall painting. Materials, techniques, analysis and conservation, Proceedings of the International Workshop, Fribourg, 7-9/03/1996* (pp. 223–235). Institute of Minerology and Petrography of Fribourg.

Boari, E., Avanzinelli, R., Melluso, L., Giordano, G., Mattei, M., De Benedetti, A. A., Morra, V., & Conticelli, S. (2009). Isotope geochemistry (Sr–Nd–Pb) and petrogenesis of leucite-bearing volcanic rocks from "Colli Albani" volcano, Roman Magmatic Province, Central Italy: Inferences on volcano evolution and magma genesis. *Bulletin of Volcanology*, *71*, 977–1005. https://doi.org/10.1007/s00445-009-0278-6

Boccalon, E., Rosi, F., Vagnini, M., & Romani, A. (2019). Multitechnique approach for unveiling the technological evolution in building materials during the Roman Imperial Age: The Atrium Vestae in Rome. *The European Physical Journal Plus*, *134*, 528. https://doi.org/10.1140/epjp/i2019-12936-y

Bonazzi, A., Santoro, S., & Mastrobattista, E. (2007). Caratterizzazione archeometrica delle malte e degli intonaci dell'Insula del Centenario. In S. Santoro (Ed.), *Pompei. Insula del Centenario (IX, 8) I. Indagini diagnostiche geofisiche e analisi archeometriche. Studi e Scavi. Nuova serie 16* (pp. 93–128). Ante Quem.

Bonetto, J., Artioli, G., Secco, M., & Addis, A. (2016). L'uso delle polveri pozzolaniche nei grandi cantieri della Gallia Cisalpina in età romana repubblicana: i casi di Aquileia e Ravenna. In J. De Laine, S. Camporeale, & A. Pizzo (Eds.), *Arqueología de la Construcción V. Man-made materials, engineering and infrastructure, Proceeding of the 5th International Workshop on the Archaeology of Roman Construction, Oxford, 11-12/04/2015, Anejos de AEspA LXXVII* (pp. 29–44). Taravilla.

Boynton, R. S. (1966). *Chemistry and technology of lime and limestone*. Wiley.

Brandon, C. J., Hohlfelder, R. L., Jackson, M. D. & Oleson, J. P. (Eds.). (2014). *Building for eternity. The history and technology of Roman concrete engineering in the sea*. Oxbow Books.

Bugini, R., & Folli, L. (2007). Le malte. In E. Roffia (Ed.), *Dalla villa romana all'abitato altomedievale. Scavi archeologici in località Faustinella-S. Cipriano a Desenzano* (pp. 78–79). Arbor Sapientiae.

Bugini, R., & Folli, L. (1993). Studio petrografico di malte e pietre. In G. Luraschi (Ed.), *Novum Comum 2050, Atti del convegno celebrativo della fondazione di Como romana, Como, 8-9/11/1991* (pp. 77–84). Società Archeologica Comense.

Buonopane, A. (1987). Estrazione, lavorazione e commercio dei materiali lapidei. In G. Cavalieri Manasse (Eds.), *Il Veneto nell'età romana* (pp. 187–213). Grafiche Fiorini.

Carulli, G. (2006). *Carta geologica del Friuli Venezia Giulia, Regione Autonoma Friuli Venezia Giulia. Scala 1:150.000*. S.El.Ca.

Carulli, G. B., & Onofri, R. (1960). *I marmi del Carso*. Regione Autonoma Friuli-Venezia Giulia.

Casadio, F., Chiari, N. G., & Simon, S. (2005). Evaluation of binder/aggregate ratios in archaeological lime mortars with carbonate aggregate: A comparative assessment of chemical, mechanical and microscopic approaches. *Archaeometry*, *47*(4), 671–689. https://doi.org/10.1111/j.1475-4754.2005.00226.x

Cinque, A., & Irollo, G. (2004). Il "Vulcano di Pompei": nuovi dati geomorfologici e stratigrafici. *Il Quaternario. Italian Journal of Quaternary Sciences*, *17*(1), 101–116.

Costa, U., Gotti, E., & Tognon, G. (2001). Nota tecnica: malte prelevate da mura antiche dallo scavo della banca popolare di Ravenna. In L. Quilici & S. Quilici Gigli (Eds.), *Fortificazioni antiche in Italia. Etá repubblicana, Atlante tematico di topografia antica 9* (pp. 25–28). L'Erma di Bretschneider.

Coutelas, A. (2012). La planification et le déroulement des chantiers de construction en Gaule romaine: l'apport de l'étude des matériaux non lithiques. In S. Camporeale, H. Dessales, & A. Pizzo (Eds.), *Arqueología de la Construcción III. Los procesos constructivos en el mundo romano: la economía de las obras, Proceedings of the 3rd International Workshop on the Archaeology of Roman Construction, Paris, 10-11/12/2009, Anejos de AEspA LXIV* (pp. 131–143). Taravilla.

Coutelas, A., Godard, G., Blanc, P., & Person, A. (2004). Les mortiers hydrauliques: synthèse bibliographique et premiers résultats sur des mortiers de Gaule romaine. *Revue d'Archéométrie*, *28*, 127–139. https://doi.org/10.3406/arsci.2004.1068

Cucchi, F., Biolchi, S., & Zini, L. (2015). Geologia e Geomorfologia del Carso Classico. In F. Cucchi, L. Zini, & C. Calligaris (Eds.), *Le acque del Carso Classico* (pp. 23–38). Edizioni Universitarie Triestine.

Cucchi, F. & Gerdol, S., (Eds.). (1985). *I marmi del Carso triestino*. Camera Commercio.

D'Ambrosio, E., Marra, F., Cavallo, A., Gaeta, M., & Ventura, G. (2015). Provenance materials for Vitruvius *harenae fossiciae* and *pulvis puteolanis*: Geochemical signature and historical-archaeological implications. *Journal of Archaeological Sciences, Reports*, *2*, 186–203. https://doi.org/10.1016/j.jasrep.2015.01.012

De'Gennaro, M., Cappelletti, P., Langella, A., Perrotta, A., & Scarpati, C. (2000). Genesis of zeolites in the Neapolitan Yellow Tuff: Geological, volcanological and mineralogical evidence. *Contributions to Mineralogy and Petrology*, *139*, 17–35.

De'Gennaro, M., Petrosino, P., Conte, M. T., Munno, R., & Colella, C. (1990). Zeolite chemistry and distribution in a Neapolitan yellow tuff deposit. *European Journal of Mineralogy*, *6*(2), 779–786.

Degryse, P., Elsen, J., & Waelkens, M. (2002). Study of ancient mortars from Sagalassos (Turkey) in view of their conservation. *Cement and Concrete Research*, *32*(9), 1457–1463.

De Luca, R., Angel, M., Cau Ontiveros, M. A., Miriello, D., Pecci, A., Le Pera, E., Bloise, A., & Crisci, G. (2013). Archaeometric study of mortars and plasters from the Roman City of Pollentia (Mallorca-Balearic Islands). *Periodico di Mineralogia*, *82*, 353–379. https://doi.org/10.2451/2013PM0021

De Luca, R., Miriello, D., Pecci, A., Domínguez-Bella, S., Bernal-Casasola, D., Cottica, D., Bloise, A., & Crisci, G. M. (2015). Archaeometric study of mortars from the Garum Shop at Pompeii, Campania, Italy. *Geoarchaeology*, *30*(4), 330–351. https://doi.org/10.1002/gea.21515

Di Girolamo, P. (1968). Un esempio di lava schiuma (*foam lava*) in Campania (lava schiuma di Pompei scavi). *Rendiconti Accademia Scienze Fisiche e Matematiche di Napoli*, *35*, 3–12.

Dilaria, S. (2020). *Malte, calcestruzzi e intonaci dipinti in Aquileia romana. Un approccio archeometrico nello studio di miscele leganti impiegate nell'edilizia antica* [PhD thesis, supervisor: Prof. J. Bonetto, University of Padova, Padova].

Dilaria, S., Addis, A., Secco, M., Bonetto, J., Artioli, G., & Salvadori, M. (2016). Vitruvian recipes in Roman Aquileia (Italy): The floor bedding mortars of Bestie Ferite and Tito Macro domus. In I. Papayianni, M. Stefanidou, & V. Pachta (Eds.), *Proceedings of the 4th Historic Mortars Conference HMC2016, Santorini, 10-12/10/2016* (pp. 145–159). RILEM Publications.

Dilaria, S., & Secco, M. (2018). Analisi archeometriche sulle miscele leganti (malte e calcestruzzi). In P. Basso (Ed.), *L'anfiteatro di Aquileia. Ricerche d'archivio e nuove indagini di scavo, Scavi di Aquileia V* (pp. 177–186). SAP edizioni.

Dilaria, S., Secco, M., Bonetto, J., & Artioli, G. (2019). Technical analysis on materials and characteristics of mortar-based compounds in Roman and Late antique Aquileia (Udine, Italy). A preliminary report of the results. In J. I. Álvarez, J. M. Fernández, Í. Navarro, A. Durán, & R. Sirera (Eds.), *Proceedings of the 5th Historic Mortars Conference HMC2019, Pamplona, 19-21/06/2019* (pp. 665–679). RILEM Publications S.A.R.L.

Di Renzo, V., Di Vito, M. A., Arienzo, I., Carandente, A., Civetta, L., D'Antonio, M., Giordano, F., Orsi, G., & Tonarini, S. (2007). Magmatic history of Somma-Vesuvius on the basis of new geochemical and isotopic data from a deep borehole (Camaldoli della Torre). *Journal of Petrology*, *48*(4), 753–784. https://doi.org/10.1093/petrology/egl081

Dunbabin, K. D. M. (1999). *Mosaics in Greek and Roman world*. Cambridge University Press.

Excoffon, P., & Dubar, M. (2011). L'Emploi de tuf volcanique et de la pouzzolane dans quelques constructions de *Forum Iulii* (Fréjus, Var). *Revue du Centre Archéologique du Var*, *2011*, 271–281.

Franzini, M., Leoni, L., & Saitta, M. (1972). A simple method to evaluate the matrix effects in X-ray fluorescence analysis. *X-Ray Spectrometry*, *1*, 151–154.

Franzini, M., Leoni, L., & Saitta, M. (1975). Revisione di una metodologia analitica per fluorescenza-X, basata sulla correzione completa degli effetti di matrice. *Rendiconti della Società Italiana di Mineralogia e Petrologia*, *31*, 365–378.

Gazzi, P., Zuffa, G. G., Gandolfi, G., & Paganelli, L. (1973). Provenienza e dispersione litoranea delle sabbie delle spiagge adriatiche fra le foci dell'Isonzo e del Foglia: inquadramento regionale. *Memorie della Società Geologica Italiana*, *12*, 1–37.

Ghedini, F., Bueno, M. & Novello, M., (Eds.). (2009). *Moenibus et portu celeberrima, Aquileia, storia di una città*. Istituto Poligrafico di Stato.

Ghiotto, A. R., Fioratto, G., & Furlan, G. (2021). Il teatro romano di Aquileia: lo scavo dell'*aditus maximus* settentrionale e dell'edificio scenico. *FOLD&R*, *495*, 1–24.

Gianfrotta, P. A. (1998). I porti dell'area flegrea. In G. Laudizi, & C. Marangio (Eds.), *Porti, approdi e linee di rotta nel Mediterraneo antico. Atti del seminario di studi, Lecce, 29-30 novembre 1996, Studi di filologia e letteratura dell'Università di Lecce, 4* (pp. 153–176). Congedo Editore.

Ginouvès, R., & Martin, R. (1985). *Dictionnaire méthodique de l'architecture grecque et romaine, Tome I, Matériaux, techniques de construction, techniques et formes du décor. Publications de l'École française de Rome 84*. Scuola tipografica S. Pio.

Gliozzo, E., & Camporeale, S. (2009). Le malte. In E. Gilozzo, I. Turbanti Memmi, A. Akerraz, & E. Papi (Eds.), *Sidi Ali Ben Ahmed—Thamusida, 2. L'archeometria* (pp. 85–118). Quasar.

Hohlfelder, R. L., & Oleson, J. P. (2014). In C. J. Brandon, R. L. Hohlfelder, M. D. Jackson, & J. P. Oleson (Eds.), *Roman maritime concrete technology in its Mediterranean context* (Vol. 2014, pp. 223–235). Oxbow books.

Jackson, M. D., Chae, S. R., Mulcahy, S. R., Meral, C., Taylor, R., Li, P., Emwas, A.-H., Moon, J., Yoon, S., Vola, G., Wenk, H.-R., & Monteiro, P. J. M. (2013). Unlocking the secrets of Al-tobermorite in Roman seawater concrete. *American Mineralogist*, *98*(10), 1669–1687. https://doi.org/10.2138/am.2013.4484

Jackson, M. D., Ciancio Rossetto, P., Kosso, C. K., Buonfiglio, M., & Marra, F. (2011). Building materials of the theatre of Marcellus, Rome. *Archaeometry*, *53*(4), 728–742. https://doi.org/10.1111/j.1475-4754.2010.00570.x

Jackson, M. D., Logan, J. M., Marra, F., Scheetz, B. E., Deocampo, D. M., & Cawood, C. G. (2011). Composizione e caratteristiche meccaniche dei calcestruzzi della Grande Aula. In L. Ungaro, M. P. Del Moro, & M. Vitti (Eds.), *I mercati di Traiano restituiti. Studi e restauri 2005-2007* (pp. 145–214). Palombi editore.

Jackson, M. D., Marra, F., Deocampo, D. M., Scheetz, B., & Vella, A. (2010). Analisi delle componenti geologiche delle murature del Foro di Cesare. *Scienze dell'Antichità. Storia, Archeologia, Antropologia*, *16*, 403–417.

Jackson, M. D., Marra, F., Deocampo, D. M., Vella, A., Kosso, C., & Hay, R. (2007). Geological observations of excavated sand (*harenae fossiciae*) used as fine aggregate in Roman pozzolanic mortars. *Journal of Roman Archaeology*, *20*, 25–53.

Jackson, M. D., Mulcahy, S. R., Chen, H., Li, Y., Li, Q., Cappelletti, P., & Wenk, H.-R. (2017). Phillipsite and Al-tobermorite mineral cements produced through low-temperature water-rock reactions in Roman marine concrete. *American Mineralogist*, *102*(7), 1435–1450. https://doi.org/10.2138/am-2017-5993CCBY

Jackson, M. D., Vola, G., Gotti, E., & Zanga, B. (2014). In C. J. Brandon, R. L. Hohlfelder, M. D. Jackson, & J. P. Oleson (Eds.), *Sea-water concretes and their material characteristics* (Vol. 2014, pp. 141–187). Oxbow books.

Katayama, T. (2010). The so-called alkali-carbonate reaction (ACR). Its mineralogical and geochemical details, with special reference to ASR. *Cement and Concrete Research*, *40*(4), 643–675. https://doi.org/10.1016/j.cemconres.2009.09.020

Kramar, S., Zalar, V., Urosevic, M., Körner, W., Mauko, A., Mirtič, B., Lux, J., & Mladenović, A. (2011). Mineralogical and microstructural studies of mortars from the bath complex of the Roman villa rustica near Mošnje (Slovenia). *Materials Characterization*, *62*(11), 1042–1057. https://doi.org/10.1016/j.matchar.2011.07.019

Lancaster, L. C. (2005). *Concrete vaulted construction in imperial rome. innovations in context*. Cambridge University Press.

Lancaster, L. C. (2006). The lightweight volcanic scoria in the concrete vaults of imperial Rome: Some evidence for trade and economy of building materials. In C. C. Mattusch, A. A. Donohue, & A. Brauer (Eds.), *Proceedings of the XVIth International Congress of Classical Archaeology, Boston, 23-26/08/2003* (pp. 212–216). Oxbow Books.

Lancaster, L. C. (2011). The use of lightweight concrete in Roma, Cilicia and Tunisia. In Å. Ringbom & R. L. Hohlfelder. (Eds.), Building Roma Aeterna: Current research on Roman mortar and concrete, *Proceedings of the Conference, Helsinki, 27-29/03/2008*, Commentationes Humanarum Litterarum 128, (pp. 60–72). Publication of the Societas Scientiarum Fennica.

Lancaster, L. C. (2015). Innovative vaulting in the architecture of the Roman Empire. *1st to 4th centuries* CE. Cambridge University Press.

Lancaster, L. C. (2019). Pozzolans in mortar in the Roman empire: An overview and thoughts on future work. In I. F. Ortega & S. Bouffier (Eds.), *Mortiers et hydraulique en Méditerranée antique, Archéologies Méditerranéennes 6* (pp. 31–39). Presses Universitaires de Provence.

Lancaster, L. C., Sottili, G., Marra, F., & Ventura, G. (2011). Provenancing of lightweight volcanic stones used in ancient Roman concrete vaulting: Evidence from Rome. *Archaeometry*, *53*(4), 707–727. https://doi.org/10.1111/j.1475-4754.2010.00565.x

Langella, A., Calcaterra, D., Cappelletti, P., Colella, A., D'Albora, M. P., Morra, V., & De'Gennaro, M. (2009). Lava stones from Neapolitan volcanic districts in the architecture of Campanian region, Italy. *Environmental Earth Sciences*, *59*, 145–160. https://doi.org/10.1007/s12665-009-0012-x

Lazzarini, L. (2006). Pietra d'Istria: genesi, proprietà e cavatura della pietra di Venezia. In N. Fiorentin, *La pietra d'Istria e Venezia, Conference proceedings, Venezia, 3 ottobre 2003* (pp. 24–45). Cierre Edizioni.

Le Bas, M. J. R., Le Maitre, W., Streckeisen, A., & Zanettin, B. (1986). IUGS subcommission on the systematics of igneous rocks, a chemical classification of volcanic rocks based on the total alkali-silica diagram. *Journal of Petrology*, *27*(3), 745–750.

Marinoni, N., Pavese, A., Foi, M., & Trombino, L. (2005). Characterisation of mortar morphology in thin sections by digital image processing. *Cement and Concrete Research*, *35*, 1613–1619. https://doi.org/10.1016/j.cemconres.2004.09.015

Marocco, R. (2009). Prima ricostruzione paleo-idrografica del territorio della bassa pianura friulano-isontina della laguna di Grado nell'Olocene. *Gortania*, *31*, 69–86.

Marra, F., Anzidei, M., Benini, A., D'Ambrosio, E., Gaeta, M., Ventura, G., & Cavallo, A. (2016). Petro-chemical features and source areas of volcanic aggregates used in ancient Roman maritime concretes. *Journal of Volcanology and Geothermal Research*, *328*, 59–69. https://doi.org/10.1016/j.jvolgeores.2016.10.005

Marra, F., & D'Ambrosio, E. (2013). Trace element classification diagrams of pyroclastic rocks from the volcanic districts of central Italy: The case study of the ancient roman ships of Pisa. *Archaeometry*, *55*(6), 993–1019. https://doi.org/10.1111/j.1475-4754.2012.00725.x

Marra, F., D'Ambrosio, E., Gaeta, M., & Mattei, M. (2016b). Petrochemical identification and insights on chronological employment of the volcanic aggregates used in ancient Roman mortars. *Archaeometry*, *58*(2), 177–200. https://doi.org/10.1111/arcm.12154

Marra, F., D'Ambrosio, E., Sottili, G., & Ventura, G. (2013). Geochemical fingerprints of volcanic materials: Identification of a pumice trade route from Pompeii to Rome. *Bulletin of the Geological Society of America*, *125*(3–4), 556–577. https://doi.org/10.1130/B30709.1

Marra, F., Deocampo, D., Jackson, M. D., & Ventura, G. (2011). The Alban Hills and Monti Sabatini volcanic products used in ancient Roman masonry (Italy): An integrated stratigraphic, archaeological, environmental and geochemical approach. *Earth Sciences Reviews*, *108*(3–4), 115–136. https://doi.org/10.1016/j.earscirev.2011.06.005

Marra, F., Karner, D. B., Freda, C., Gaeta, M., & Renne, P. (2009). Large mafic eruptions at Alban Hills Volcanic District (Central Italy): Chronostratigraphy, petrography and eruptive behavior. *Journal of Volcanology and Geothermal Research*, *179*(3–4), 217–232. https://doi.org/10.1016/j.jvolgeores.2008.11.009

Matschei, T., Lothenbach, B., & Glasser, F. P. (2007). The AFm phase in Portland cement. *Cement and Concrete Research*, *37*, 118–130. https://doi.org/10.1016/j.cemconres.2006.10.010

Miriello, D., Barca, D., Bloise, A., Ciarallo, A., Crisci, G. M., De Rose, T., Gattuso, C., Gazineo, F., & La Russa, M. F. (2010). Characterisation of archaeological mortars from Pompeii (Campania, Italy) and identification of construction phases by compositional data analysis. *Journal of Archaeological Sciences*, *37*(9), 2207–2223. https://doi.org/10.1016/j.jas.2010.03.019

Miriello, D., Bloise, A., Crisci, G. M., Apollaro, C., & La Marca, A. (2011). Characterisation of archaeological mortars and plasters from Kyme (Turkey). *Journal of Archaeological Science*, *38*, 794–804. https://doi.org/10.1016/j.jas.2010.11.002

Miriello, D., Bloise, A., Crisci, G. M., De Luca, R., De Nigris, B., Martellone, A., Osanna, M., Pace, R., Pecci, A., & Ruggieri, N. (2018). New compositional data on ancient mortars and plasters from *Pompeii* (Campania—Southern Italy): Archaeometric results and considerations about their time evolution. *Materials Characterization*, *146*, 189–203. https://doi.org/10.1016/j.matchar.2018.09.046

Miriello, D., & Crisci, G. M. (2006). Image analysis and flatbed scanners. A visual procedure in order to study the macro-porosity of the

archaeological and historical mortars. *Journal of Cultural Heritage*, *7*(3), 186–192. https://doi.org/10.1016/j.culher.2006.03.003

Mogetta, M. (2015). A new date for concrete in Rome. *Journal of Roman Studies*, *105*, 1–40. https://doi.org/10.1017/S007543581500043X

Montana, G., Randazzo, L., Ventura-Bordenca, C., Giarrusso, R., Baldassarri, R., & Polito, A. M. (2018). The production cycle of lime-based plasters in the Late Roman settlement of Scauri, on the island of Pantelleria, Italy. *Geoarchaeology*, *34*, 631–647. https://doi.org/10.1002/gea.21697

Moore, R. E. M. (1968). A newly observed stratum in Roman floor mosaics. *American Journal of Archaeology*, *72*(1), 57–68.

Morandeau, A., Thiery, M., & Dangla, P. (2014). Investigation of the carbonation mechanism of {CH} and C-S-H in terms of kinetics, microstructure changes and moisture properties. *Cement and Concrete Research*, *56*, 153–170. https://doi.org/10.1016/j.cemconres.2013.11.015

Morra, V., Calcaterra, D., Cappelletti, P., Colella, A., Fedele, L., De'Gennaro, R., Langella, A., Mercurio, M., & De'Gennaro, M. (2010). Urban geology: Relationships between geological setting and architectural heritage of the Neapolitan area. In M. Beltrando, A. Peccerillo, M. Mattei, S. Conticelli, & C. Doglioni (Eds.), *Journal of the Virtual Explorer*, *36*(26), 1–60. https://doi.org/10.3809/jvirtex.2010.00261

Munsell, A. (1994). *Soil color charts* (rev. ed.). Munsell Publishing Company.

Navrátilová, E., & Rovnaníková, P. (2016). Pozzolanic properties of brick powders and their effect on the properties of modified lime mortars. *Construction and Building Materials*, *120*, 530–539. https://doi.org/10.1016/j.conbuildmat.2016.05.062

Novello, M. (2017) I mosaici di Aquileia in età tardoantica. In F. Ghedini, M. Bueno, M. Novello, & F. Rinaldi (Eds.), I mosaici di Aquileia in età tardoantica I pavimenti romani di Aquileia, Contesti, Tecniche, Repertorio decorativo, *Antenor Quaderni 37/1–2* (pp. 519–533). Padova University Press.

Papayianni, I., Pachta, V., & Stefanidou, M. (2013). Analysis of ancient mortars and design of compatible repair mortars: The case study of Odeion of the archaeological site of Dion. *Construction and Building Materials*, *40*, 84–92. https://doi.org/10.1016/j.conbuildmat.2012.09.086

Peccerillo, A. (2005). *Plio-quaternary volcanism in Italy: Petrology, geochemistry*. Springer.

Pecchioni, E., Fratini, F., & Cantisani, E. (2014). *Atlante delle malte antiche in sezione sottile al microscopio ottico*. Nardini.

Piovesan, R., Curti, E., Grifa, C., Maritan, L., & Mazzoli, C. (2009). Ancient plaster technology: Petrographic and microstratigraphic analysis of plaster-based building materials from the Temple of Venus, Pompeii. *Interpreting silent artefacts: Petrographic approaches to archaeological ceramics* (pp. 65–79). Archaeopress.

Previato, C. (2015). Aquileia. Materiali, forme e sistemi costruttivi dall'età repubblicana alla tarda età, *Antenor Quaderni 32*. Padova University Press.

Rebecchi, F. (1980). Sull'origine dell'insediamento in Grado e sul suo porto tardo-antico. Grado nella storia e nell'arte, Atti della X Settimana di Studi Aquileiesi, Aquileia, 28/04-4/05 1979, Antichità Altoadriatiche 17/1 (pp. 41–56), Arti Grafiche Friulane.

Rispoli, C., De Bonis, A., Esposito, R., Sossio, F. G., Langella, A., Mercurio, M., Morra, V., & Cappelletti, P. (2020). Unveiling the secrets of Roman craftsmanship: Mortars from Piscina Mirabilis (Campi Flegrei, Italy). *Archaeological and Anthropological Sciences*, *12*, 8. https://doi.org/10.1007/s12520-019-00964-8

Rispoli, C., De Bonis, A., Guarino, V., Sossio, F. G., Di Benedetto, C., Esposito, R., Morra, V., & Cappelletti, P. (2019). The ancient pozzolanic mortars of the thermal complex of Baia (Campi Flegrei, Italy). *Journal of Cultural Heritage*, *40*, 143–154. https://doi.org/10.1016/j.culher.2019.05.010

Rochelle, C. A., Milodowski, A. E., Bateman, K., Moyce, E. B. A., & Kilpatrick, A. (2016). A long-term experimental study of the reactivity of basement rock with highly alkaline cement waters: Reactions over the first 15 months. *Mineralogical Magazine*, *80*(6), 1089–1113. https://doi.org/10.1180/minmag.2016.080.056

Roffia, E., Bugini, R., & Folli, L. (2009). Stone material of the Roman villas around Lake Garda (Italy). ASMOSIA VII, *Proceedings of the 7th International Conference of the Association for the Study of Marble and Other Stones in Antiquity, Thasos, 15-20/09/2003, Bulletin the Correspondence Hellénique supplementary 51*, (pp. 559–570), Publications de École Française.

Rubinich, M. (2012a). Intonaci dipinti dall'area delle "Grandi Terme" di Aquileia: rapporto preliminare. In F. Oriolo & M. Verzár-Bass (Eds.), *La pittura romana nell'Italia settentrionale e nelle regioni limitrofe, Atti della XLI settimana di studi aquileiesi, Aquileia, 6-8/05/2010, Antichità altoadriatiche 73* (pp. 233–240). Editreg.

Rubinich, M. (2012b). Dalle "Grandi Terme" alla "Braida Murada": storie di una trasformazione. In J. Bonetto & M. Salvadori (Eds.), *L'architettura privata ad Aquileia in età romana, Atti del Convegno di Studi, Padova, 21-22/02/2011, Antenor Quaderni 24* (pp. 619–637). Padova University Press.

Rubinich, M. (2013). Le Thermae Felices Constantinianae. In C. Tiussi, L. Villa, & M. Novello (Eds.), *Costantino e Teodoro. Aquileia nel IV secolo, Exhibition Catalog, Aquileia, 5/07-3/11/2013* (pp. 85–90). Electa.

Rubinich, M. (2014). Le Grandi Terme Costantiniane. *Aquileia Nostra, LXXXIII-LXXXIV/2012-2013*, 97–117.

Rubinich, M. (2018). Adduzione e distribuzione delle acque nelle 'Grandi Terme' di Aquileia: i dati dello scavo. In G. Cuscito (Ed.), *Cura Aquarum, adduzione e distribuzione dell'acqua nell'antichità, Atti della XLVIII settimana di studi aquileiesi, Aquileia, 10-12/05/2017, Antichità altoadriatiche 88* (pp. 87–106). Editreg.

Rubinich, M. (2020). Le grandi terme di Aquileia: passato, presente e futuro di un edificio pubblico tardoantico. *Quaderni Friulani di Archeologia*, *30*, 71–90.

Russell, B. (2013). *The economics of the Roman stone trade*. Oxford University Press.

Santacroce, R. (1987). *Somma-Vesuvio*. Consiglio nazionale delle ricerche.

Santacroce, R., Cioni, R., Marianelli, P., Sbrana, A., Sulpizio, R., Zanchetta, G., Donahue, D. J., & Joron, J. L. (2008). Age and whole rock-glass compositions of proximal pyroclastics from the major explosive eruptions of Somma-Vesuvius: A review as a tool for distal tephrostratigraphy. *Journal of Volcanology and Geothermal Research*, *177*(1), 1–18. https://doi.org/10.1016/j.jvolgeores.2008.06.009

Schmolder-Veit, A., Thiemann, L., Henke, F., & Schlutter, F. (2019). Hydraulic mortars in the imperial residence. An interdisciplinary project on the Platine/Rome. In I. F. Ortega & S. Bouffier (Eds.), *Mortiers et hydraulique en Méditerranée antique, Archéologies Méditerranéennes 6* (pp. 31–39). Presses Universitaires de Provence.

Schneider, C. A., Rasband, W. S., & Eliceiri, K. W. (2012). NIH Image to ImageJ: 25 years of image analysis. *Nature Methods*, *9*, 671–675. https://doi.org/10.1038/nmeth.2089

Secco, M., Dilaria, S., Addis, A., Bonetto, J., Artioli, G., & Salvadori, M. (2018). Evolution of the Vitruvian recipes over 500 years of floor making techniques: The case studies of *Domus* delle Bestie Ferite and *Domus* di Tito Macro (Aquileia, Italy). *Archaeometry*, *60*(2), 185–206. https://doi.org/10.1111/arcm.12305

Secco, M., Dilaria, S., Bonetto, J., Addis, A., Tamburini, S., Preto, N., Ricci, G., & Artioli, G. (2020). Technological transfers in the Mediterranean on the verge of the Romanization: Insights from the waterproofing renders of Nora (Sardinia, Italy). *Journal of Cultural Heritage*, *44*, 63–82. https://doi.org/10.1016/j.culher.2020.01.010

Secco, M., Previato, C., Addis, A., Zago, G., Kamsteeg, A., Dilaria, S., Canovaro, C., Artioli, G., & Bonetto, J. (2019). Mineralogical

clustering of the structural mortars from the Sarno Baths, Pompeii: A tool to interpret construction techniques and relative chronologies. *Journal of Cultural Heritage*, *40*, 265–273. https://doi.org/10.1016/j.culher.2019.04.016

Silva, D. A., Wenk, H. R., & Monteiro, P. J. M. (2005). Comparative investigation of mortars from Roman Colosseum and cistern. *Thermochimica Acta*, *438*, 35–40. https://doi.org/10.1016/j.virol.2005.03.003

Stanislao, C., Rispoli, C., Vola, G., Cappelletti, P., Morra, V., & Gennaro, M. (2011). Contribution to the knowledge of ancient Roman seawater concretes: Phlegrean pozzolan adopted in the construction of the harbour at Soli-Pompeiopolis (Mersin, Turkey). *Periodico di Mineralogia*, *80*, 471–488. https://doi.org/10.2451/2011PM0031

Stefanidou, M., Pachta, V., Konopissi, S., Karkadelidou, F., & Papayianni, I. (2014). Analysis and characterization of hydraulic mortars from ancient cisterns and baths in Greece. *Materials and Structures*, *47*, 571–580. https://doi.org/10.1617/s11527-013-0080-y

Tentor, M., Tunis, G., & Venturini, S. (1994). Schema stratigrafico e tettonico del Carso isontino. *Natura Nascosta*, *9*, 1–32.

Teutonico, J. M., Ashall, G., Garrod, E., & Yates, T. (2000). A comparative study of hydraulic lime-based mortars. In P. Bartos, C. Groot, & J. J. Hughes (Eds.), *Historic mortars: Characteristics and tests, Proceedings of the International RILEM workshop, Paisley, 12-14/05/1999* (pp. 339–349). RILEM publications.

Thiery, M., Villain, G., Dangla, P., & Platret, G. (2007). Investigation of the carbonation front shape on cementitious materials: Effects of the chemical kinetics. *Cement and Concrete Research*, *37*(7), 1047–1058. https://doi.org/10.1016/j.cemconres.2007.04.002

Vola, G., Gotti, E., Brandon, C., Oleson, J. P., & Hohlfelder, R. L. (2011). Chemical, mineralogical and petrographic characterization of Roman ancient hydraulic concretes cores from Santa Liberata, Italy, and *Caesarea Palestinae*, Israel. *Periodico di Mineralogia*, *80*(2), 317–338. https://doi.org/10.2451/2011PM0023

Wentworth, C. K. (1922). A scale of grade and class terms for clastic sediment. *Journal of Geology*, *30*(5), 377–392.

Zacharopoulou, G. (2009). Interpreting chemistry and technology of lime binders and implementing it in the conservation field. *Conservar Património*, *10*, 41–53.

SUPPORTING INFORMATION

Additional supporting information may be found in the online version of the article at the publisher's website.

How to cite this article: Dilaria, S., Secco, M., Rubinich, M., Bonetto, J., Miriello, D., Barca, D., & Artioli, G. (2022). High-performing mortar-based materials from the late imperial baths of Aquileia: An outstanding example of Roman building tradition in Northern Italy. *Geoarchaeology*, 37, 637–657. https://doi.org/10.1002/gea.21908